Tampereen yliopisto

Topias Lilja

PREPARATION AND CHARACTERIZATION OF INJECTABLE CHITOSAN/BIOACTIVE GLASS CEMENTS FOR MINIMALLY INVASIVE TREATMENT OF BONE DEFECTS

Faculty of Engineering and Natural Sciences
Master of Science Thesis
4/2024

ABSTRACT

Topias Lilja: Preparation and Characterization of Injectable Chitosan/Bioactive Glass Cements For Minimally Invasive Treatment of Bone Defects
Master of Science Thesis
Tampere University
Master's Programme in Materials Engineering
4/2024

Bone Tissue Engineering is a rapidly growing field of study, which focuses on developing alternative treatment to help in the reconstruction of bone defects with critical size. The use of autograft (bone harvested from the patient) has remained the "golden standard" in bone reconstruction. However, limitations in donor tissue availability as well as the need for a surgical operation at the donor site, leading to long recovery times and post-operative pain, are the main disadvantages of such procedure. High interest has been given to reducing invasiveness of surgical procedures leading to the development of injectable bone substitutes (IBS). They are cements with paste-like consistency and have an ability of setting *in vivo,* after injection, into the bone defect site. IBS consists of a liquid phase (natural or synthetic polymer -based liquid), and a powder phase (ceramics, bioactive glass or glass ceramic) in proportion resulting in optimal injectability, mechanical properties, rheology, and bioactivity. Like any other bone substitute material, IBS is promoting new bone formation and is degrading gradually *in vivo*, being replaced by the newly formed tissue.

The aim of this thesis was to study and prepare two different compositions of injectable bone cements using one commercially available bioactive glass, S53P4 silicate glass and one experimental bioresorbable calcium phosphate glass (PhGlass), as powder phase. The liquid phase consisted of chitosan and citric acid. The first developed composition had only S53P4 as powder phase, while the second composition consisted of 50 wt% S53P4 and 50 wt% PhGlass, with particle sizes <38 µm. Liquid phase was an aqueous solution of 2-wt% of chitosan and 20 wt% of citric acid. In addition, the other aim of the study was to build an injectability testing set up using standard mechanical testing device and ordinary laboratory equipment with better repeatability compared to injectability testing by hand, which was successfully done with few limitations.

Injectability of both compositions was first evaluated by preparing the cements with different L/S-ratios, putting them into 2 ml syringe and by studying the amount of injected paste as function of setting time. The most suitable L/S-ratios for both cements were chosen based on their injectability behavior and setting times. The criteria for proper injectability were paste-like consistency combined with high ratio of extruded paste through the syringe as well as ease of injecting the cement by hand. 0.75 ml/g L/S-ratio was chosen for both cements to be used in the next phases.

Mechanical properties of cements were studied by compression test of cylindrical hardened samples of both conditions, prior immersion in SBF. The compression test showed that the cement with both glasses had better mechanical properties, in general, compared to the one with only S53P4. Both cements withstood compressive strength relatively well despite early-stage crack propagation in the test.

In vitro dissolution was studied by soaking the samples in SBF for up to 1 week at 37 °C, under 100 RPM agitation. The mass loss, post-immersion was evaluated, as well as change in the SBF pH. In addition, concentrations of dissolved ions in SBF were analyzed by ICP-OES. Furthermore, samples with different immersion times were analyzed by SEM-EDX. It was found that the major part of the PhGlass had dissolved into SBF after 1 week of immersion which decreased the pH due to high release of phosphorus. ICP suggested that a reactive HA-like layer was precipitating in both cements, which could be confirmed by SEM-EDX analysis in case of the cement with mixed glasses, but not with the S53P4/chitosan -cement. SEM-EDX also showed indications of reactive layer formation both on the surface of the cement and inside the cement cylinder.

As a conclusion, both cements showed promising performance to be used in IBS applications, but further investigations are needed, mainly considering setting times and cytotoxicity.

Key words: bone tissue engineering, bone cement, bioactive glass, chitosan, composite

TIIVISTELMÄ

Topias Lilja: Injektoitavien kitosaani/bioaktiivinen lasi -sementtien valmistaminen ja karakterisointi minimaalisesti invasiiviseen luuvaurioiden hoitoon
Diplomityö
Tampereen Yliopisto
Materiaalitekniikan DI-ohjelma
4/2024

Luukudosteknologia on nopeasti kasvava tieteenala, joka keskittyy kehittämään vaihtoehtoisia menetelmiä luuvaurioiden hoitoon. Luukudos on rakenteeltaan ja ominaisuuksiltaan ainutlaatuinen ja monimutkainen kudostyyppi. Tämän takia autografti -luusiirteet ovat säilyneet ”kultaisena standardina” luukudoksen rekonstruktiossa. Joka tapauksessa, luovutuskudosten saatavuudessa ilmenee rajoitteita ja perinteisten luusiirteiden tekeminen vaatii suuria kirurgisia toimenpiteitä, mikä aiheuttaa potilaille suurta kipua ja pitkiä toipumisaikoja. Leikkaushoitona suoritettavien toimenpiteiden vähentäminen on nykyisin tärkeä tavoite lääketieteen sovelluksissa, mikä on johtanut myös injektoitavien luuta korvaavien materiaalien (engl. IBS) kehittämiseen. Ne ovat tahnamaisia sementtejä, joilla on kyky kovettua elimistössä sen jälkeen, kun ne ovat injektoitu luuvaurion alueelle. Injektoitavat luusementit koostuvat nestemäisestä faasista (luonnon/synteettinen polymeeri) ja jauhe/partikkelifaasista (bioaktiivinen lasi/lasikeraami). Molemmat faasit yhdessä muodostavat optimaalisen ominaisuusyhdistelmän luusementtiin mm. injektoitavuuden, mekaanisten ja reologisten ominaisuuksien sekä bioaktiivisuuden näkökulmasta. Injektoitavat luusementit tarjoavat sopivan ympäristön uuden luukudoksen muodostumiselle ja hajoavat vähitellen elimistössä terveen luun korvatessa ne.

Diplomityöni tarkoituksina oli valmistella erilaisia luusementtejä luusovelluksissa käytettävistä bioaktiivisista laseista sekä arvioida niiden soveltuvuutta käytettäväksi injektoitavissa luusementeissä eri tutkimusmenetelmien perusteella. Työssä käytettiin jo kaupallistettua S53P4 silikaattilasia ja kokeellista kalsiumfosfaattilasia. Ensimmäisessä sementissä jauhefaasina oli S53P4, ja toisessa sekoitus 50 paino-% S53P4-lasia ja 50 paino-% kalsiumfosfaattilasia partikkelikoossa <38 µm. Nestemäisenä faasina molemmissa oli kaksi paino-% kitosaania ja 20 paino-% sitruunahappoa sisältävä vesiliuos. Lisäksi työssä rakennettiin injektoitavuuden testauslaitteisto käyttäen standardista mekaanista testauslaitetta sekä tavanomaista laboratoriovälineistöä, mikä saatiin toteutettua onnistuneesti.

Sementtien injektoitavuutta arvioitiin puristamalla niitä eri liuos/jauhe -suhteilla 2 ml ruiskun läpi ja mittaamalla ruiskun läpi tulleen sementin määrää kovettumisajan funktiona. Molemmille sementeille valittiin liuos/jauhe -suhteeksi 0,75 ml/g injektoitumiskäyttäytymisen ja kovettumisaikojen perusteella tutkittavaksi tarkemmin. Mekaanisia ominaisuuksia tutkittiin suorittamalla kovettuneille sylinterimäisille näytteille kompressiotesti. Sementti, joka sisälsi molempia laseja, osoittautui mekaanisesti vahvemmaksi. Sen keskimääräinen kimmomoduli oli 123 MPa ja korkein kompressiojännitys 15 MPa, kun vastaavat arvot S53P4 -lasia sisältäneelle sementille olivat järjestyksessä 68 MPa ja 10 MPa. Siitä huolimatta molemmat sementit kestivät hyvin kompressiokuormitusta, vaikka halkeamia alkoi ydintyä näytteisiin testin aikana.

Sementtien hydrolyyttistä hajoamista tutkittiin upottamalla näytteet SBF-liuokseen yhdeksi viikoksi 37 °C:ssa. Massan ja pH:n muutosta tarkkailtiin ajan funktiona ja näytteistä liuenneiden ionien konsentraatioita tutkittiin ICP-OES:n avulla. Lisäksi näytteiden pintaa ja läpileikkausta tutkittiin SEM-EDX:lla. Huomattiin, että kalsiumfosfaattilasi liukeni lähes kokonaan viikon aikana, mikä nosti liuoksen pH-arvoa vapautuneen fosforin määrän takia. ICP-tulosten perusteella arvioitiin, että reaktiivinen apatiittikerrostuma muodostui molempien sementtien pinnalle. Havainto pystyttiin todentamaan SEM-EDX analyysin perusteella molempia laseja sisältäneen sementin kohdalla.

Johtopäätöksenä voidaan todeta, että molemmat sementit osoittivat lupaavaa toiminnallisuutta käytettäväksi injektoitavissa luusementeissä. Tulevaisuudessa on kuitenkin tärkeää tutkia lisää sementtien kovettumisaikojen muokattavuutta. Lisäksi on varmistettava, ettei sementeistä vapaudu elimistöön liian suuria määriä ioneja, jotka saattavat olla soluille myrkyllisiä korkeissa konsentraatioissa.

Avainsanat: luukudosteknologia, luusementti, bioaktiivinen lasi, kitosaani, komposiitti

PREFACE

This document template conforms to the Guide to Writing a Thesis in Technical Fields at Tampere University (2023).

I want to thank my supervisor, Professor Jonathan Massera, for giving me an opportunity to work in his great research group during my thesis project and for supporting me during the work.

I also want to say big thanks to Postdoctoral Researcher Amel Houaoui and Doctoral Researchers Agata Szczodra, Jenna Tainio, Sonya Ghanavati, and Virginia Alessandra Gobbo for giving me guidance in sample preparation and characterization throughout the laboratory experiments.

Tampere, 15.4.2024

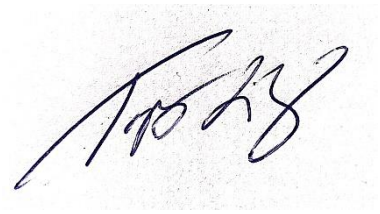

Topias Lilja

TABLE OF CONTENTS

TABLE OF FIGURES

LIST OF ABBREVIATIONS

BAG	Bioactive glass
BTE	Bone tissue engineering
$(BO_3)^{3-}$	Borate ion
B_2O_3	Boron trioxide
β-TCP	β- tricalcium phosphate
$CaCl_2 \cdot 2H_2O$	Calcium chloride dihydrate
$CaCO_3$	Calcium carbonate
$(CaHPO_4) \cdot 2H_2O$	Dicalcium phosphate dihydrate
CaO	Calcium oxide
$Ca(PO_3)_2$	Calcium phosphite
Ca^{2+}	Calcium ion
$Ca_{10}(PO_4)_6(OH)_2$	Chemical formula of hydroxyapatite crystals
$(CH_2OH)_3CNH_2$	Tris(hydroxymethyl)aminomethane
$(CO_3)^{2-}$	Carbonate ion
CuO	Copper oxide
EDS/EDX	Energy dispersive spectroscopy
HA	Hydroxyapatite
HCA	Hydroxyl carbonate apatite
HCl	Hydrochloric acid
H^+	Hydrogen ion
H_3BO_3	Boric acid
HNO_3	Nitric acid
H_3O^+	Oxonium ion
IBS	Injectable bone substitute
ICP-OES	Inductively coupled plasma – optical emission spectroscopy
in vitro	In a test tube, culture dish etc., outside a living organism
in vivo	In a living organism
KCl	Potassium chloride
$K_2HPO_4 \cdot 3H_2O$	Dipotassium hydrogen phosphate trihydrate
L/S -ratio	Liquid to solid -ratio
$MgCl_2 \cdot 6H_2O$	Magnesium dichloride hexahydrate
MgO	Magnesium oxide
MnO	Manganese oxide
mol%	Mole percentage
Na^+	Sodium ion
NaCl	Sodium chloride
Na_2CO_3	Sodium carbonate
$NaHCO_3$	Sodium bicarbonate
Na_2O	Sodium oxide
$NaPO_3$	Sodium hexametaphosphate
Na_2SO_4	Sodium sulphate
NH_6PO_4	Ammonium phosphate
NiO	Nickel oxide
PhGlass	Phosphate glass
$(PO_4)^{3-}$	Phosphate ion
P_2O_5	Phosphorus pentoxide
RPM	Rounds per minute
RT	Room temperature
SD	Standard deviation
SEM	Scanning electron microscopy
SG	Silicate glass
SiO_2	Silica (silicon dioxide)

$Si(OH)_4$	Silicic acid
$SrCO_3$	Strontium carbonate
SrO	Strontium oxide
S53P4	A composition of silicate bioactive glass
TiO_2	Titanium dioxide
wt-%	weight percentage
13-93	A composition of silicate bioactive glass
13-93B20	A composition of borosilicate bioactive glass
3D	Three-dimensional
45S5	A composition of silicate bioactive glass

1. INTRODUCTION

Bone tissue engineering (BTE) is a rapidly growing field of study, developing alternative therapies for all kinds of bone defects, such as fractures, tumor resection, bone infections and bone diseases such as osteoporosis. (Bloise et al., 2021). BTE aims at creating a combination of materials and biological properties to build an optimal environment to promote bone tissue growth and proper healing of the defect. New engineered treatment methods are needed due to limitations and drawbacks in conventional “golden standard”. Indeed, the use of autografts is associated with low donor tissue availability, low cost-effectiveness, side effects, and errors in normal remodeling of the bone. (Bloise et al., 2021.) Additionally, autografting requires several surgical operations, when the donor tissue is taken from one part of the body and grafted to another, leading to donor site morbidity (Khoshakhlagh et al., 2017).

Reducing the invasiveness of surgical procedures has been a major topic. Additionally, conventional orthopedic implants have their disadvantages in fitting them into differently shaped bone defects, which can lead to bone loss or trauma to the surrounding tissue or even poor/incomplete bone healing. This has resulted in development of injectable bone substitutes (IBS), which has opened the path toward minimally invasive surgeries, where bone cements are injected inside the bone defect/cavity. The viscous paste has the ability of filling those cavities of different shapes and hardening *in situ* after injection. Thus, long recovery times and post operative pain can be reduced significantly and make surgical procedures easier, while preventing healing of large wounds and muscle damage. (Khoshakhlagh et al., 2017; Song et al., 2009; Lima et al., 2020.)

The physiological performance and environment of bone are setting certain requirements for bone substitute materials. As previously investigated in my bachelor’s thesis work, bone substitute materials should be biocompatible and biodegradable and have suitable mechanical properties in relation to the substitutive bone tissue type. Biodegradation rate of the bone substitute material should match the bone regeneration rate. Thus, the bone substitute material must provide mechanical support to the damaged bone tissue while degrading *in vivo.* (Lilja, 2022.) In the context of this work, the bone substitute materials should also have good injectability and suitable rheological properties to be able to fill randomly shaped bone cavities in their entirety and flow through thin syringes.

The aim of this thesis work was to investigate the suitability of silicate (S53P4) and calcium phosphate (CaP) bioactive glasses mixed with chitosan and citric acid to form injectable composite bone substitutes. The liquid to solid ratio was varied and the impact of inorganic content, on the setting of the cement, assessed by injectability test. Mechanical properties, *in vitro* dissolution, and bioactive properties were assessed on cements with optimized liquid to solid ratio. Based on test results, different composite mixtures were evaluated for their suitability to fit in applications where injectable bone substitute systems could be beneficial. Additionally, the other aim of this work was to build an injectability testing set up with good repeatability using standard mechanical testing device and ordinary laboratory equipment.

2. THEORETICAL BACKGROUND

In this chapter, relevant literature on the topic is covered including, bone structure and properties, composite materials as bone substitutes and state of the art in injectable bone substitutes. In addition, materials used in the manufacturing of the composite bone cements investigated in the experimental part of the thesis, are introduced.

2.1 Bone

Bone can be described as a composite material composed of fibrous protein, collagen, stiffened by surrounding crystals of calcium phosphate (Currey, 2013). Additionally, there are also many more constituents included in bone tissue, such as many proteins, polysaccharides, and water. Also, blood vessels and living cells are present in many types of bone. (Currey, 2013.) On the other hand, bone is a mineralized connective tissue with four types of bone cells which are bone lining cells, osteoblasts, osteocytes, and osteoclasts, all of which have their own important function in the bone remodeling process (Florencio-Silva et al., 2015).

According to John D. Currey, *bone-lining cells* are forming thin continuous sheets to cover all bone surfaces. These surfaces control the movement of ions from body to bones and vice-versa. *Osteoblasts* are cells derived from bone-lining cells, whose primary role is to form new bone during skeletal development and remodeling. They lay down new bone, *osteoid,* which is a matrix derived from collagen and other proteins. In osteoid, the bone mineral is later mineralized. (Currey, 2013.) *Osteocytes* are bone cells located in mineralized bone matrix and they have crucial role in detecting bone damages in the matrix and initiating responses of bone repair. Osteocytes have also many more important functions in bone, such as converting mechanical stimuli into biochemical reactions and cell response (mechanotransduction), regulating calcium homeostasis and serum phosphate levels as well as energy storage and use. (Zreiqat et al., 2015.) The last bone cell type, *osteoclasts,* are bone-resorbing cells. They are multinucleated cells originated from hematopoietic stem cell lineage. (Currey, 2013; Florencio-Silva et al., 2015.) Mature osteoblasts can attach to bone surface and secrete hydrochloric acid (HCl) and proteolytic enzymes. The acid causes dissolution of hydroxyapatite (HA) which allows proteolytic enzymes to access the bone matrix and start to degrade it. (Ralston, 2021.)

Bones have several important functions in the body. They provide structural support to soft tissues, protect organs from external hazards, enable locomotion of the body in co-operation with muscles and tendons, act as phosphate and calcium storage, and harbor bone marrow inside them. (Florencio-Silva et al., 2015.)

2.1.1 Structure and properties

Bone matrix is a complex and highly organized network of organic and inorganic segments. Organic segments account for approximately 30% of the bone volume and they consist of collagenous proteins (90%) such as type I collagen and non-collagenous proteins, bone morphogenetic proteins and growth factors. (Bloise et al., 2021.) The organic matrix covers about 25% of the bone weight and promotes elasticity and tensile strength of bone (Granke et al., 2015).

Inorganic matrix of bone primarily consists of hydroxyapatite (HA) crystals ($Ca_{10}(PO_4)_6(OH)_2$), which are hexagonally organized crystals storing 99% of calcium, 85% of phosphorous, and 40-60% of sodium and magnesium of the human body (Bloise et al., 2021). The hydroxyapatite mineral accounts for about 65% of the bone weight and provides rigidity to bone (Ralston, 2021; Bloise et al., 2021). The rest of the inorganic segment consists of ions such as citrate, carbonate, bicarbonate, potassium, zinc, and barium (Bloise et al., 2021). The rest of the weight of bone is water, which is shown to improve fracture toughness properties of bone tissue. Water is essentially existing in two compartments in bones: bound in the bone matrix (bound water) and within pores (pore water). The pore water of the bone is shown to be an important factor leading to elastic properties. This is mainly attributable to the collagen ductility. The bound water on the contrary, is affecting mainly to the post-yield properties of bone by providing ductility to collagen. (Granke et al., 2015.) Mechanical properties of bone can be seen in Table 1.

There are two main structural types of bone (Figure 1.): i.e. cortical and trabecular bone (Ralston, 2021). Cortical bone is a dense bone type that has low surface area with overall porosity in the range of only 2-12 % (Gerhardt & Boccaccini, 2010; Fu et al., 2011). Cortical bone forms a cover to bone marrow cavity and consist of *Haversian systems* (also called as osteons). Haversian system is a cylindrically shaped structure consisting of lamellae of bone tissue, which acts as an envelope to the central canal, where blood vessels and nerve fibers are located. Haversian systems are aligned parallel to the bone axis. (Ralston, 2021.)

Table 1. *Mechanical properties of bone found from literature. (Gerhardt & Boccaccini, 2010; Fu et al., 2011)*

Property	Trabecular bone	Cortical bone
Tensile strength (MPa)	1-5	50-151
Young's Modulus (GPa)	0.05-5	7-30
Compressive strength (MPa)	2-12	100-150
Fracture toughness (MPa·$m^{1/2}$)	0.1-0.8	5-10
Bending strength (MPa)	10-20	135-193
Porosity (%)	50-90	2-12

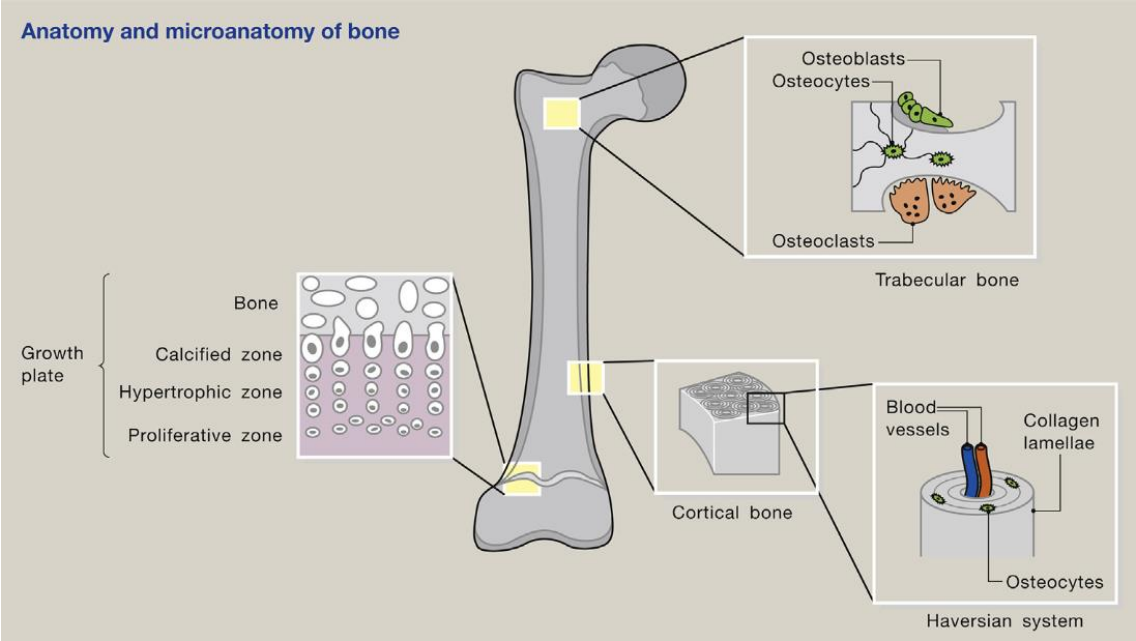

Figure 1. *Schematic picture of bone anatomy. In addition, locations of trabecular and cortical bone are indicated (Ralston, 2021).*

All bones, in the body, are covered by an outer shell of cortical bone (Reznikov, 2014). Trabecular bone (also called as spongy or cancellous bone), has lower density and surface area compared to cortical bone (Ralston, 2021). It is highly interconnected porous bone generally found in the inner parts of bones, filling up either the entire inner volume of bone (i.e., vertebrae and ribs) or being present only partially in some parts of the bone (i.e., epiphyses of long bones). The overall porosity of trabecular bone is in the range of 50-90 % with pore size >500 µm. (Gerhardt & Boccaccini, 2010; Fu et al., 2011; Reznikov,2014.)

2.1.2 Bone healing

Bone healing is a very complex process where several different tissues, cells and signaling pathways are involved in partially overlapping cascades, finally resulting in a new regenerated bone tissue. Figure 2 gives more detailed information about the different phases of the bone healing process and involved tissues and cells, as well as covers requirements for the biomaterial to support natural bone healing. (Winkler et al., 2018.)

Bone healing process proceeds in the following manner. When bone defect occurs, the disrupted blood vessels are causing the formation of hematoma, which initiates an immune response at the defect site. This inflammatory reaction acts as an initiator of the bone healing process. (Schmidt-Bleek et al., 2012.) At the end of the inflammatory phase, the hematoma starts to mature towards granulation tissue, removing cellular debris. The granulation tissue transforms into reparative callus tissue, which is mainly consisting of cartilage. The soft callus tissue is mineralized and transformed into hard callus, where development of woven bone is occurring, replacing the cartilage. After that, bone remodeling occurs based on the mechanical stimulation sensed by the tissue due to the strains caused by movement of the limb. This restores the original mechanical properties of the bone. (Winkler et al., 2018.)

When designing a bone healing implant, an injectable bone cement system in case of this thesis work, remodeling of bone regulated by mechanosensing needs to be taken into consideration properly. The biomaterial should not be stiffer than the repaired bone tissue in order to transfer the mechanical stimulation to the bone. It has been shown that mechanical stimulation increases bone formation and lack thereof results in bone loss, at the biomaterial-bone interface and loosening of the implanted material. This phenomenon is called stress-shielding. Hence, early-stage weight bearing of bone after fracture/defect has been found to be effective and it has become a standard clinical practice nowadays. (Winkler et.al., 2018.)

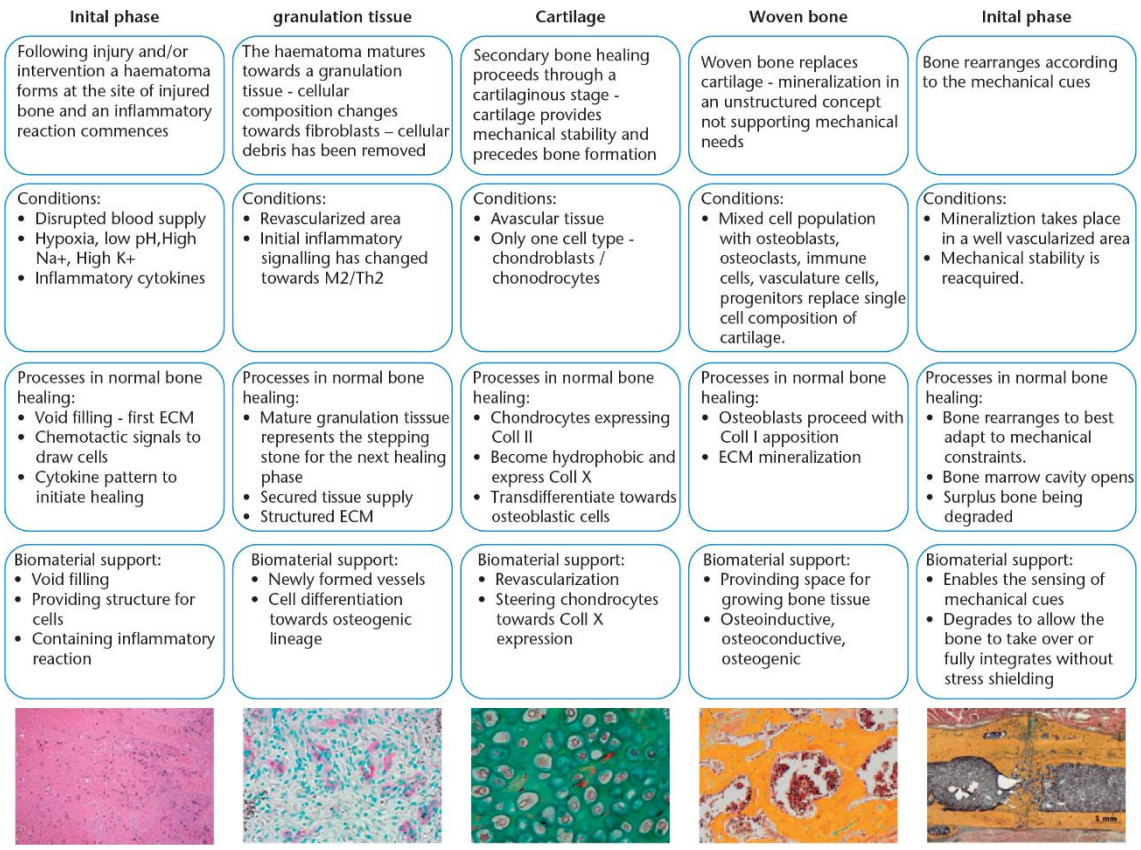

Figure 2. *Phases of bone healing, as well as biomaterials characteristics, and requirements in different phases of the healing process (Winkler et al., 2018).*

Additionally, bone voids caused by tumor or tumor-like lesions are aimed to be treated with bone substitute materials. The most effective filler material is still autologous bone graft, but calcium phosphate ceramics, especially β-tricalcium phosphate (β-TCP), have been shown to be potential bone graft substitute materials when autologous bone grafts are not available in sufficient quantity. In case of bone voids, degradation of the biomaterial and new bone formation are starting from the periphery of the defect, proceeding towards the inner volume of the defects. The most important factors that are affecting the quality of bone void healing are oxygen and nutrient supply throughout the defect. Therefore, fibrous tissue formation inside the void and reinforcing the angiogenesis are critical factors, at least in case of larger defects. There are some promising tissue engineering approaches to overcome those requirements in bone void healing including gene therapy and special matrices. (Kucera et al., 2011.)

2.2 Chitosan

Chitosan is a commonly used biomaterial which is derived from chitin, a linear polysaccharide occurring naturally in crab and shrimp shells. Chitin consists of repeating units of N-acetyl-D-glucosamine and its structure can be seen in Figure 3. Chitin has potential to be used in biomedical applications but its insolubility in water and other commonly used solvents has been a major problem that has prevented its use in the medical field. Hence, many kinds of approaches have been studied aiming to increase chitin's solubility in water. One approach, i.e. deacetylation of chitin via alkaline treatment, has turned out to be the most used method these days. Chitosan is a derivative of chitin which has a degree of deacetylation in the range 30-95%. (Dutta, 2016; Sergi et al., 2020.)

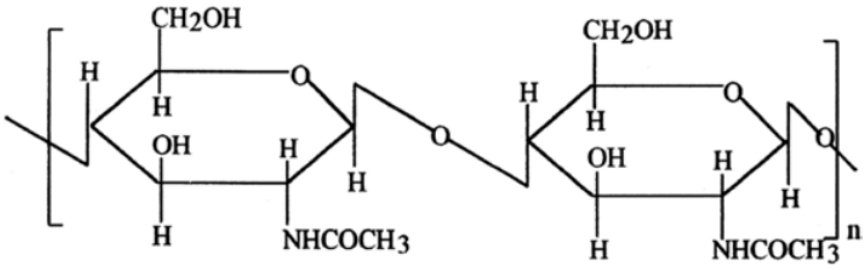

Figure 3. *Repeating units of N-acetyl-D-glucosamine in chitin (Dutta, 2016).*

As a result of a previous study, it was noticed that the best osteogenic effect and highest volume of new bone regeneration was achieved with chitin derivatives with deacetylation of 50-70 % . The deacetylation reaction of chitin can be seen in Figure 4. Thus, chitosan is a copolymer consisting of N-acetyl-D-glucosamine units and deacetylated D-glucosamine units. Chitosan is soluble in aqueous acidic solutions. (Dutta, 2016.)

According to Dutta's book, it has been investigated that the degree of deacetylation affects the physicochemical and biological performance of chitosan. The higher degree of deacetylation chitosan has, the better it dissolves in water due to higher exposure of positively charged amine groups in the glucosamine units. (Dutta, 2016.) However, biocompatibility of chitosan is decreasing with increasing degree of deacetylation, solubility, and degradation rate. In addition, chitosan can be fully dissolved only in diluted acid (pH<6). (Sergi et al., 2020.)

Chitosan is said to be the second most abundant biopolymer in nature after cellulose, so its availability is high (Bloise et al., 2020).

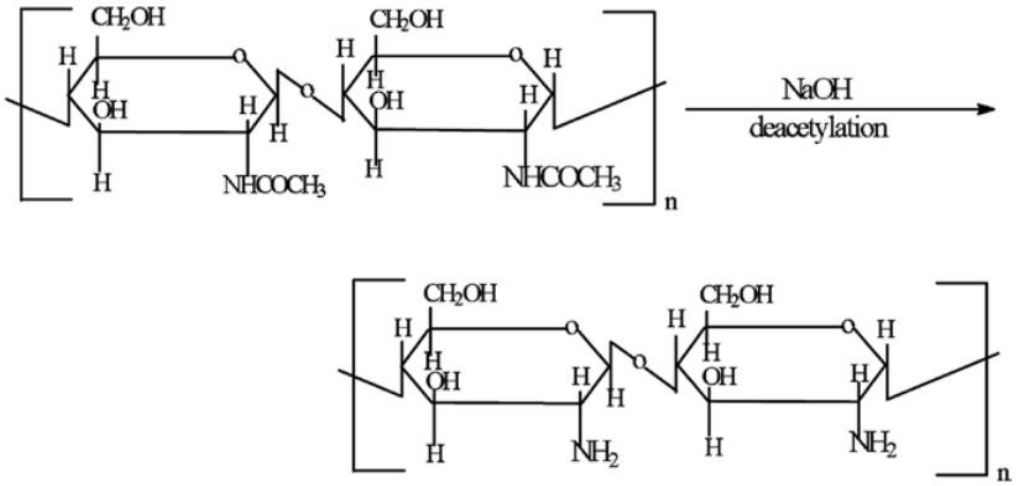

Figure 4. *Deacetylation of chitin into chitosan (Dutta, 2016).*

In addition, chitosan is a highly biocompatible and biodegradable natural biopolymer. It has been found to be a very promising material from its osteogenic properties. Several studies have demonstrated that chitosan is able to promote stem cell differentiation into osteoblasts, supporting new bone formation as well as growth of bone cell colonies *in vitro*. According to literature, this performance is assigned to the amine and hydroxylic groups of chitosan. Additionally, the chemical backbone of chitosan mimics glycosaminoglycan which is the major component of bone and cartilage. Therefore, chitosan is a material with high potential in bone applications. (Bloise et al., 2020; Sergi et al., 2020.)

Chitosan has also low toxicity, good antibacterial properties and it can be used in manufacturing composite for tissue engineering scaffolds such as hydrogels, fibrous matrices, and open pore materials (Costa-Pinto et al., 2014). Even though the mechanism that causes the antimicrobial effect of chitosan is not completely understood, it is suggested that the negative charge of chitosan is affecting the ability of bacteria to penetrate tissue membranes. The other possible factor might be that chitosan can bond with bacterial DNA and inhibit their RNA synthesis. (Sergi et al., 2020.)

Chitosan based hybrid materials have been shown to have good swelling ability, mechanical properties, compression modulus and improved microstructure in bone, nerve, cartilage, liver, and musculoskeletal tissue regeneration, for instance (Dutta, 2016). Furthermore, chitosan has shown ability of promoting wound healing, inhibiting infection, and activating macrophages to produce cytokines, modulating the immune

system (Costa-Pinto et al., 2014). Chitosan degrades mainly enzymatically by lysozymes *in vivo* (Costa-Pinto et al., 2014; Dutta, 2016). Lysozymes are enzymes which can be found in many fluids of human body, such as tears, saliva, serum, and fluids surrounding cartilage. Neutrophils and macrophages are releasing lysozymes during inflammation. It has been proven that the degree of acetylation of chitosan is inversely proportional to the degradation kinetic. (Costa-Pinto et al., 2014.)

2.3 Bioactive glass

Glass has an amorphous structure (Figure 5) and, as such, does not have long-range periodic crystalline structure and is often prepared as a mixture of three different component types (Brauer, 2015). *Network formers such as* silica (SiO_2), boron trioxide (B_2O_3), and phosphorus pentoxide (P_2O_5), are components which can form glass structure without any additional components by bridging oxygen atoms. *Network modifiers* can change the glass structure by turning the bridging oxygen atoms into non-bridging oxygen atoms. Network modifiers are usually oxides of alkali metals, such as sodium (Na) or potassium (K) or alkaline earth metals such as calcium (Ca). The last component type, *intermediate oxides,* can theoretically act either like network formers by entering the backbone of the glass network, or network modifiers by turning the bridging oxygen atoms into non-bridging oxygens. (Brauer, 2015.)

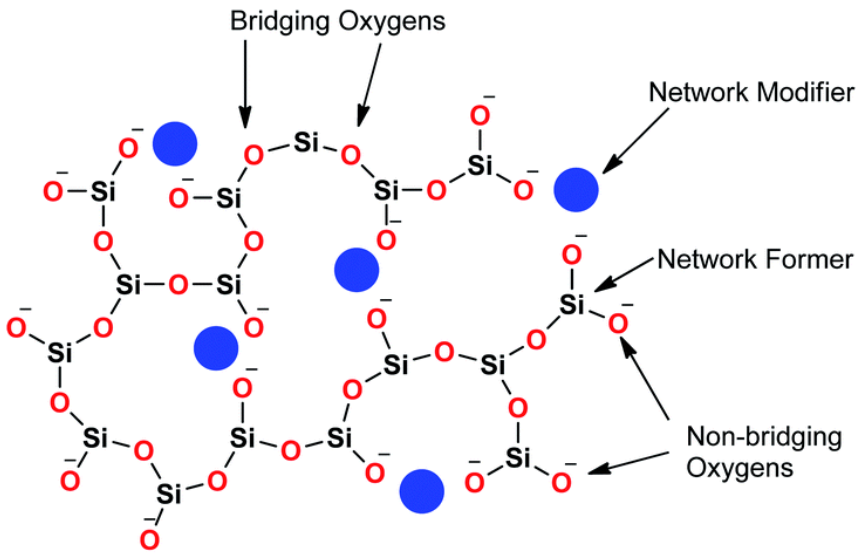

Figure 5. *Schematic illustration of bioactive glass structure composed of silicate backbone (Deshmukh et al., 2020).*

Bioactive glasses (BAG) are very interesting materials for bone tissue engineering due to their unique properties (Kaur, 2017). Their composition is easy to adjust to be suitable for different purposes. BAGs promote differentiation of mesenchymal stem cells, osteoblast adhesion and enzyme activity. Furthermore, BAGs can enhance revascularization, which is crucial for the successful bone tissue regeneration and proper healing of the tissue. (Kaur, 2017.) BAGs are both osteoinductive and osteoconductive materials (Houaoui et al., 2021). Osteoinductivity refers to the ability of inducing differentiation and proliferation of stem cells into osteogenic cells, whereas osteoconductivity means that the material provides a suitable environment for the bone to grow. The newly formed tissue is tightly bonded with the surface of the material (Ghassemi et al., 2018).

Larry L. Hench et al. introduced a pioneering definition of a bioactive material: “a bioactive material is one that elicits a specific biological response at the interface of the material which results in the formation of a bond between the tissues and the material” (Hench et al., 2013). After implantation into the body, bioactive material forms a biological interface of hydroxyapatite like layer, which is important in soft and hard tissue interactions (Kaur, 2017). In case of bioactive glasses, this apatite layer is formed due to release of ions such as calcium and phosphate during the dissolution of bioactive glass in body fluids (Brauer, 2015). The interface forming onto the surface of the biomaterial is a biologically active layer of hydroxyl carbonate apatite (HCA). The HCA layer structure and composition is similar to the mineral phase of bone. (Marchi, 2016.)

BAGs are hard and brittle materials with relatively low fracture toughness, but their Young’s modulus is high and comparable to bone, which is an advantage as a bone substitute material (Kaur, 2017). Tensile bending strength of most conventional BAGs is said to be approximately 40-60 MPa, which prevents their use in load-bearing applications. Nevertheless, bioactive glasses can be utilized in bioactive coatings, low-load and compression loaded applications as well as in composites, as the bioactive phase. The major advantage of bioactive glasses as bone substitute materials is their bone bonding property, which is attributed to the chemical reactivity of the glass in body fluids (Hench et al., 2013).

The first bioactive glass ever developed was introduced by Larry L. Hench in 1969. It was named as 45S5 and its composition was 46.1 mol% SiO_2, 2.6 mol% P_2O_5, 24.4 mol% Na_2O and 26.9 mol% CaO. Most bioactive glasses used in modern regenerative medicine are composed of different concentrations of these same components as in the 45S5 BAG. (Brauer, 2015.) According to Hench’s et al., bioactive glasses differ from

other bioactive ceramics by the possibility to control their chemical properties as well as their rate of bonding to hard tissues. Thus, bioactive glasses are easy to design very specifically to a certain biomedical application. (Hench et al., 2013.)

BAGs can be manufactured with two different methods: Conventional melt-quenching method, where glass is formed by mixing different precursors via a melting/quenching process. Sol-gel method, is a more modern and complex way, where solution (sol) composed of metal-organic and metal salt precursors is firstly synthesized. In a second time, the solution is going through a gelation process by chemical reaction or alternatively aggregation. Finally, the gel is treated thermally to dry the gel, remove organics and sometimes to obtain crystallization as well. (Nandi et al., 2011.)

2.3.1 Silicate Bioactive Glasses

The structure of silicate glasses (SG) is a network of tetrahedral silicon-oxygen blocks (Figure 6.), where the Si-O bonds angles can vary from 120° to 180° (Brauer, 2015; Kaur 2017). Silicate glasses have quite open structure, which is a result of each oxygen anion being coordinated with two silicon cations leading to corner sharing of the tetrahedral structure (Marchi, 2016). Properties of SGs depends on the alkali and earth-alkali metals, contents and composition, which converts the bridging oxygen atoms into non-bridging oxygens, causing disruption of the glass network connectivity and opening-up the structure. The quantity of non-bridging oxygen atoms and the strength of metal-oxygen bonds are affecting viscosity and chemical durability properties of the silicate glass. (Nandi et al., 2011.)

There are many silicate bioactive glass compositions used in different bone applications nowadays, some of which can be seen in Table 2. Silicate bioactive glasses have been shown to promote stem cell differentiation into osteoblasts and thus, enhancing the new bone regeneration (Bianco et al, 2013). Additionally, their degradation by-products have been found to induce neovascularization, promoting angiogenesis, *in vitro*. In addition, the degradation by-products promote bone growth by affecting the gene expression of osteoblasts. (Bianco et al., 2013.) 3D porous structure is the optimum shape for bone graft and that can be obtained via ceramic sintering. However, in case of silicates, sintering can lead to uncontrolled crystallization which tends to have a negative effect on bioactive properties. (Gerhardt & Boccaccini, 2010; Kaur, 2017.)

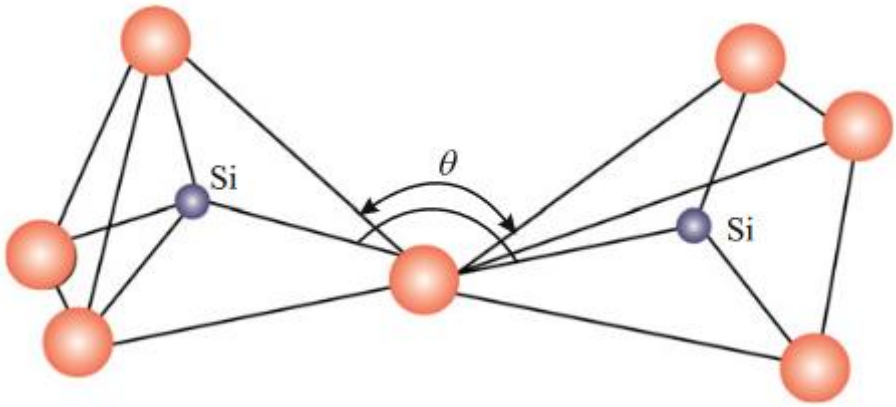

Figure 6. *Silicon-oxygen block, a basic building block of silicate glasses (Kaur, 2017).*

Table 2. *Silicate bioactive glass compositions (mol%). Adapted from (Brauer et. al, 2015).*

	SiO_2	P_2O_5	Na_2O	CaO	CaF_2	K_2O	MgO
45S5	46.1	2.6	24.4	26.9	-	-	-
S53P4	53.9	1.7	22.7	21.8	-	-	-
13-93	54.6	1.7	6	22.1	-	7.9	7.7

Silicate bioactive glasses are studied to be degrading incongruently in aqueous solutions. According to Larry L. Hench, dissolution of silicate glass in aqueous solution occurs as follow:

1. Rapid ion exchange between the network modifiers (alkali and alkaline earth elements) with H^+ or H_3O^+ from the solution occurs. Secondly, silanol groups (Si-OH) are forming at the glass surface via hydrolysis of silica groups. The interfacial pH increases due to H^+ consumption in the reaction.

$$Si - O - Na^+ + H^+ + OH^- \rightarrow Si - OH^+ + Na^+(aq) + OH^-$$

2. Silica network starts to break by the attack of hydroxyl ions (hydrolysis), resulting in release of silicic acid ($Si(OH)_4$) into the solution. Additionally, formation of silanol groups started in phase 1 is continuing at the surface of the BAG.

$$Si - O - Si + H_2O \rightarrow Si - OH + OH - Si$$

3. Silica-rich layer depleted in alkali and alkaline earth cations is forming onto the glass surface through polycondensation of neighboring silanols.

4. Migration of calcium (Ca^{2+}) and phosphate ions ($(PO_4)^{3-}$) through the silica-rich layer from both dissolving glass and the solution leads to precipitation of amorphous calcium phosphate (CaP) layer at the surface.

5. The amorphous calcium phosphate layer crystallizes by incorporating carbonate anions ($(CO_3)^{2-}$) from the solution resulting in a hydroxyl carbonate apatite layer. (Hench, 1998; Nandi et al., 2011.)

Silicate BAG composition S53P4 (composition can be seen in Table 2.) has been shown to have good osteoconductive, angiogenetic and antibacterial properties (Romano et. al., 2014). It can facilitate tissue ingrowth, thereby enhancing formation of new bone. Studies have shown, that S53P4 releases sodium, phosphorus , and calcium ions during degradation in body fluids, which causes increase in pH and osmotic pressure. This leads to an environment which is hostile to proliferation of bacterial pathogens and their adhesion, giving antibacterial properties to the glass. S53P4 (BonAlive, Bonalive Biomaterials Ltd, Finland) has been given approval as medical device in Europe and it is used in treatment of osteomyelitis. (Romano et. al., 2014.)

Borosilicate glasses are significantly more reactive and chemically less durable, which results in faster degradation and conversion to HA compared to their silica counterparts. On the other hand, borosilicate glasses have improved thermal properties, making them optimum for the processing of scaffolds (Marchi, 2016). Borosilicate glasses have also shown to promote cell differentiation and proliferation *in vitro* as well as tissue infiltration *in vivo*. However, some studies have indicated toxicity of borate ions ($(BO_3)^{3-}$) and cytotoxic performance of some borosilicate glass compositions in static conditions *in vitro*. These toxic performances can be inhibited by pre-incubation, using dynamic cell cultures, or converting the glass partially to HA in advance before placing it to the tissue culture. (Marchi, 2016.)

Borosilicate glass 13-93B20 is a bioactive glass based on 13-93 silicate composition in which 20% of the SiO_2 is substituted with B2O3. Borosilicate compositions of 13-93 BAG are investigated to degrade faster *in vitro* compared to 13-93. Additionally, they have shown faster conversion to HA, while still having slower degradation kinetics than silicate compositions S53P4 and 45S5. (Houaoui et al., 2021.)

2.3.2 Phosphate bioactive glasses

Phosphate based bioactive glasses have been introduced in the biomedical field over 40 years ago. Phosphorus pentoxide (P_2O_5) acts as a network former oxide in phosphate glasses. The basic building block in phosphate glasses is a phosphate tetrahedra (Figure 7.) which are bonding with each other to form the network (Kaur, 2017). There are several possible forms of phosphate tetrahedra in phosphate networks, which can be seen in Figure 7. Different tetrahedra are varying by the number of bridging oxygen atoms. Phosphate glasses are mainly consisting of Q^3 (branching unit), Q^2 (middle unit), Q^1 (end unit), and Q^0 (isolated orthophosphate group). The Q^i terminology is used in classification of the phosphate tetrahedra, where "i" is indicating the number of bridging oxygens per tetrahedron. Compared to silica 3D network, phosphate tetrahedra can attach to 3 neighboring tetrahedra, whereas silicate has 4 attachment opportunities at most. (Brow, 2000.)

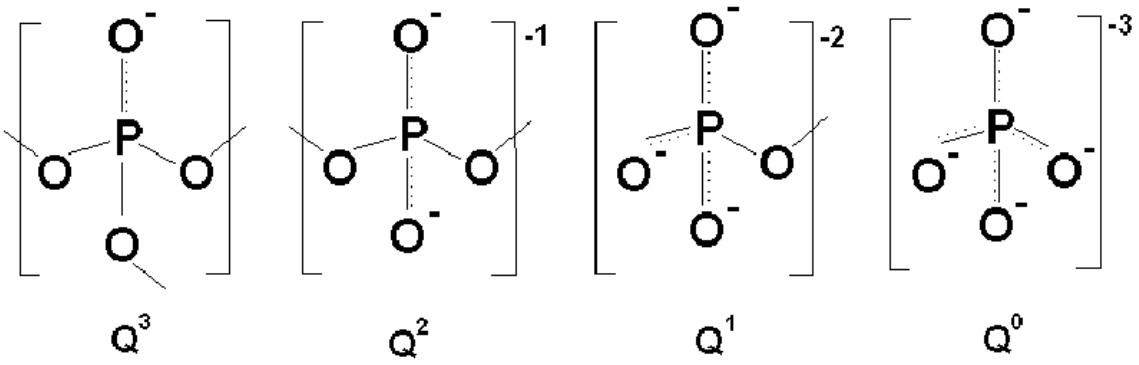

Figure 7. *Different phosphate tetrahedra existing in structure of phosphate bioactive glasses (Lakshmikanta et. al., 2012).*

The field of biomaterials engineering is usually focusing mainly on development of invert phosphate glasses, which have P content of <40 mol% (Ghanavati et. al., 2023). They degrade incongruently and have ability to promote cell adhesion, differentiation and proliferation as well as form a reactive layer of CaP upon immersion in body fluids. However, the tendency of crystallization upon heat treatment is a major drawback, making invert phosphate glasses impossible to use as sintered BAG based scaffolds. Metaphosphates on the other hand, with P_2O_5 content of more than 50%, made of Q^2 phosphate chains, are interesting materials due to the congruent dissolution which makes them potential vehicles in controlled delivery of therapeutic ions. Fast dissolution of metaphosphate glasses in body fluids usually leads to poor cell viability, but this limitation can be overcome by changing the composition and decreasing the dissolution rate. (Ghanavati et. al., 2023.)

Generally accepted theory considering phosphate glass dissolution in aqueous solutions (Figure 8.) can be represented as follow (Gao et.al., 2000):

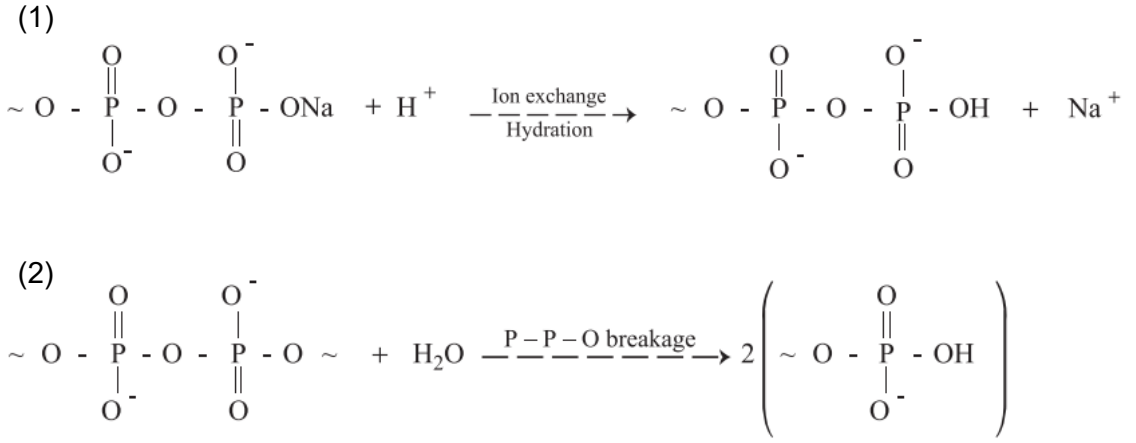

Figure 8. *Two phases of phosphate glass dissolution in aqueous solutions. (Gao et al., 2004)*

(1) Hydration reaction: Exchange of Na^+ ion from the glass and H^+ ion from the solution, which is resulting in a formation of a hydrated layer on the surface of the phosphate glass at the interface of glass and solution.

(2) Network breaks: In hydrated layer, P-O-P bonds break under the attack of H^+ ions and water molecules. This leads to breakage of glass network and phosphate chains are released into the solution with different degrees of polymerization.

The reactive calcium phosphate layer formation in body fluids by phosphate glasses is very complex process compared to silica, but the few studies carried out on the topic have given promising information that suggests that phosphate can facilitate bone mineralization. It has been a general hypothesis, that high phosphate content in bioactive glasses promotes calcium-phosphate formation and osteogenesis *in vitro* as well as *in vivo*. As a result of Li's et. al. study, it was discovered that high phosphate content in BAG led to faster formation of a reactive layer and better promotion of osteogenesis as well as higher bioactivity. (Li et.al., 2021.)

The phosphate tetrahedra is very asymmetric in nature, which causes low chemical durability as well as sensitivity to hydration of P-O-P bonds. Nevertheless, phosphate glasses are very interesting materials in regenerative medicine due to ease of tailoring the dissolution properties by adding metal oxides to the composition such as TiO_2, MnO, NiO and CuO. (Kaur, 2017.) By changing the composition, it is possible to tailor the dissolution time of phosphate glasses from a couple of days to years. In addition, the dissolution mechanism in phosphate glasses can be significantly different depending on the P to Ca ratio. With different P to Ca ratios, phosphate glasses can dissolve either congruently or incongruently. (Ghanavati et. al., 2023.)

Phosphate glasses have been studied for application of controlled release of antibacterial ions such as zinc, silver, and copper. They can be used in various soft and hard tissue applications due to the versatility and ease of tailoring the properties. In addition, phosphate glasses are widely used to fabricate glass fibers for many biomedical applications. (Kaur, 2017.) Nevertheless, there are still few limitations and challenges in using phosphate glasses in bone applications considering particle migration, settling and handleability. In addition, they have poor flexibility and fatigue strength alone, and therefore they cannot be used in load bearing applications. (Killion et. al, 2013.)

2.4 BAG/Natural polymer composites in bone regenerative medicine

Biomaterials have specific requirements which must be fulfilled before they can be used in biomedical applications. They must be biocompatible, non-toxic, non-allergenic and non-carcinogenic. Biomaterials can be classified by their response to the host tissue after implantation into the body. (Sergi et.al., 2020.) For the first-generation biomaterials, the most important design requirements were biocompatibility and inertness, in order to avoid foreign body reactions. In addition, these materials should provide sufficient

mechanical support to the damaged tissue during the healing process (Kaur, 2017.) These biomaterials do not cause chemical or biological changes in the host tissue nor do they change biologically or chemically inside the body. Second-generation biomaterials, on the other hand, have the ability of promoting a certain biological response on its surface. In case of bone applications, second-generation biomaterials can induce controlled reaction mechanisms in physiological environment of bone to stimulate bone formation. The last group, third-generation biomaterials have, additionally to the second-generations biomaterials, the ability of promoting specific responses also at a molecular level. (Sergi et.al., 2020.)

Composites are defined as materials in which two or more constituents with different physical and/or chemical properties are combined to form a unique mixture with improved properties and performance compared to the individual components (Bloise et al., 2021; Gu et al., 2018). When composites are used as biomaterials in biomedical applications, they are often called biocomposites. Biocomposites consist of two phases, matrix and reinforcement. The matrix is usually either synthetic or natural polymeric materials or resins, which are reinforced with fibers or particles. The reinforcement phase can vary from natural or synthetic fibers to bioceramic particles. The matrix phase holds the reinforcement phase together, transferring the stresses from the environment to the reinforcement, hence achieving mechanically strong and functional biomaterial combination. (Elnashar et. al., 2023; Gu et al., 2018.) Hybrid materials are differing from composites by the fact that they are not just a simple physical mixture of two phases. In hybrid materials, two or more materials are connected to each other at the nanoscale or molecular level, creating combinations of new properties by chemical and physical properties of individual components and the interfaces between these components. (Gu et. al., 2018.)

Based on previous literature covering bone regenerative medicine, limitations in properties of BAGs and natural polymers alone can be overcome by introducing BAG particles into natural polymeric systems. In BAG/natural polymer composites, the polymeric phase provides the required plasticity and toughness properties to the composite. BAGs, on another hand, promote compressive strength and mineralization properties, the second of which are associated with the composites bioactivity. (Killion et. al., 2013.) Additionally, according to Khoshakhlagh's et al. study, BAG/chitosan composites were showing higher cellular viability and better bone formation with higher ratio of BAG particles. Also, it was found that degradation rate of the composite and cellular viability could be controlled by adjusting the content of particles in the composite.

(Khoshakhlagh et.al., 2017.) The ease of tailoring chemical composition of BAGs by adding ions (network modifier) into their structure also provides tools for stimulating different cellular responses in the host tissue (Sergi et al., 2020).

As a result of another previous study, carried out at Tampere University, Faculty of Medicine and Health Technology, *in vitro* evaluation of S53P4/Chitosan porous scaffolds was promising toward hard tissue applications. The scaffold induced CaP reactive layer precipitation which suggests bioactivity. Also, effect of introducing the BAG particles to chitosan on the mechanical properties of the scaffold was studied and it was discovered that the presence of BAG particles increased slightly the mechanical properties. This was thought to be associated with the high cross-linking of the chitosan, induced by ionic interaction of leached ions and the hydrated layer on the glass surface. Additionally, best mechanical properties were said not to be achieved with highest load of BAG particles due to agglomeration of glass particles, decreasing the homogeneity of structure and properties of the composite scaffold. (Faqhiri et. al., 2019.)

2.5 Introduction to injectable bone substitutes (IBS)

Conventional graft reconstruction is often used when it comes to administration of bone substitutes. This requires relatively major surgical operations which can cause infections and high post-operative pain as well as retraction of large muscles. (Sadiasa et. al., 2014.) In orthopedics, research has been focusing on reducing the invasiveness of operations, where biomaterials are implanted into the wound site to substitute bone voids or damaged tissue (Lima et al., 2020). One of the most important advancements in treatment of non-load bearing bone defects has been the development of injectable bone cement system (Figure 9.) (Song et al., 2008).

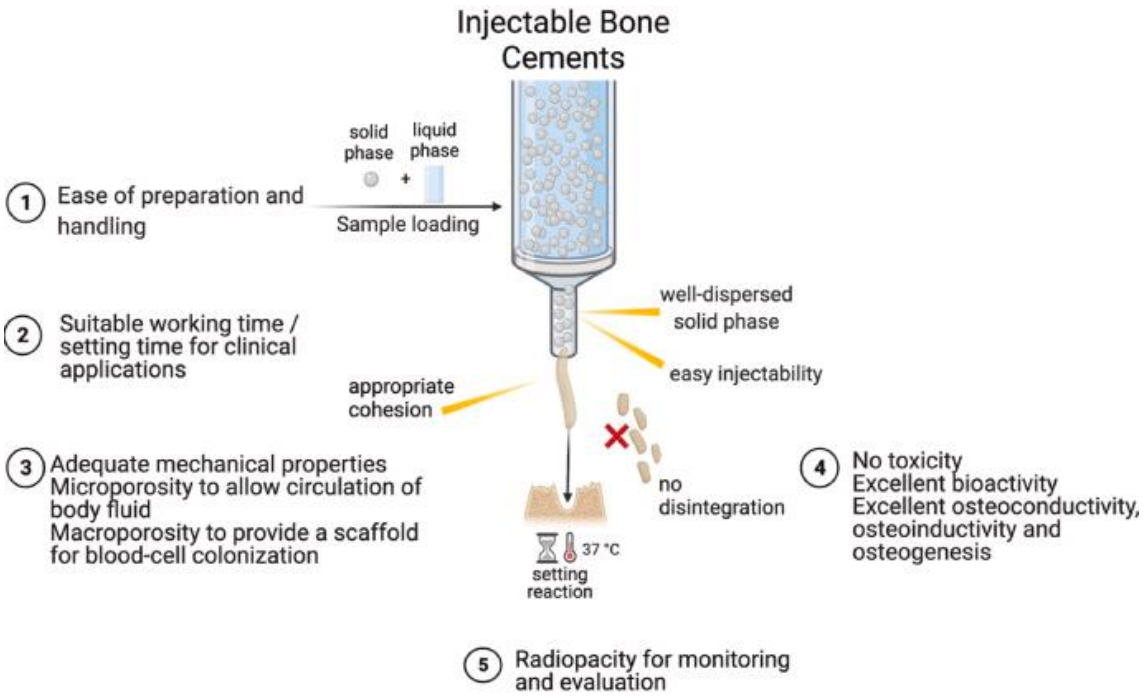

Figure 9. Schematic illustration of IBS system and requirements (Demir-Oğuz et. al., 2023).

It is based on minimally invasive technique in which bone cements are injected into the bone cavities. Injectable cements have suitable properties to mold into randomly shaped bone cavities and set in situ after injection. This kind of system is beneficial compared to a conventional hardened orthopedic implant due to shorter surgical operation times and decrease in scar size and post-operative pain to the patient. With minimally invasive bone substitutes, fast recovery of the bone is possible to achieve with relatively low cost. (Song et al., 2008.)

In year 1986, biomaterial scientists called Brown and Chow developed a revolutionary formulation of calcium phosphate bone cement, which was composed of tetracalcium phosphate and dicalciumphosphate dihydrate (Sadiasa et. al., 2014). Further development of this formulation led to major advancements in application of IBS, providing self-setting abilities, reasonable injectability properties, moldability, high reactivity with bone and applicability in controlled drug delivery. The trend of using nature-derived materials for their biocompatibility and properties of promoting faster healing in implantable applications, led to the introduction of those materials into IBS systems, such as chitosan, citric acid, sodium alginate, collagen, gelatin, hyaluronic acid, and derivatives of cellulose has been used as liquid phase in IBS. Chitosan and citric acid are the most widely used nature-derived substances in IBS due to their good biocompatibility. Additionally, citric acid is known to enhance injectability of IBS and

influence bone formation by absorbing Ca^{+} ions, being an ingredient of human hard tissue. However, several studies have shown that biocompatibility of IBSs needs to be further developed, especially because high concentrations of citric acid might delay the apatite formation and cause inflammatory reaction *in vivo.* In addition to calcium phosphate, also silicate bioactive glasses have been interesting biomaterials in field of IBS. They are potential materials in bone grafting applications due to their ability of promoting bone formation and bonding to bone via HCA layer formation in body fluids, while dissolving over time. (Sadiasa et. al., 2014.)

There are several properties IBS is required to have to achieve optimal success in surgical operation as well as proper tissue healing. Injectability refers to the ability of the bone cement paste to extrude out from the syringe, while keeping its homogenic consistency. There is not a standard method of measuring injectability, but usually it's defined according to the force needed to extrude the paste or by assessing the mass of material extruded as a function of setting time. (Demir-Oğuz et. al., 2023.) Robinson et. al created a protocol, where injectability can be evaluated by using standard mechanical tester. This protocol generates a force vs. displacement graph from the measurement data from which the injectability behavior of every individual sample can be evaluated (Figure 10). (Robinson et. al., 2020.)

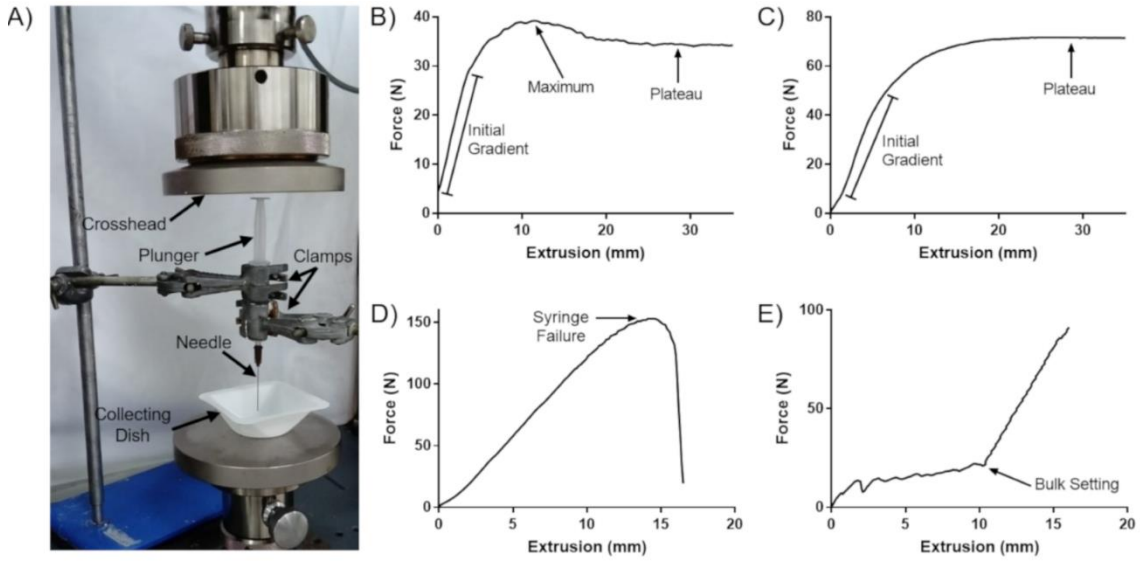

Figure 10. *Force-displacement curves of different injectability behaviors in injectability test based on mechanical tester (Robinson et al., 2021).*

Other important requirements for IBSs, besides injectability, are biocompatibility and bioactivity, ease of shaping and moldability as well as setting under physiological conditions. Setting should occur within 15 minutes of IBS preparation to avoid wash out of the cement in body fluids, but not too fast so that the surgeon has enough time to do the procedure. In addition, too fast setting of the cement might lead to poor filling of the defect. After setting, IBS should provide sufficient microporosity for angiogenesis, as well as microporosity to allow transportation of body fluids and nutrients through the structure of the cement. The rheological and mechanical properties should be similar to the bone tissue which is replaced by the IBS. To avoid disintegration of the cement particles from the injection site, sufficient cohesiveness should be reached against the surrounding fluid. As these cements are easily washed out when getting in touch with body fluids, disintegrated cement particles could easily end up in bloodstream and cause damage via vascular blockage. They could also cause inflammatory reaction and cell necrosis near the injection site. As IBS is implanted via minimally invasive procedure, also radiopacity is required for the surgeon to be able to correctly position the cement at the injection site. In addition, radiopacity of the IBS is also important factor in monitoring the defect during and after the procedure as well as in case of potential failure. (Demir-Oğuz et. al., 2023.)

3. MATERIALS AND METHODS

This chapter covers all materials, sample preparation and testing methods used in this thesis work. In the experimental part of the thesis, two different composite cements were prepared with different liquid (chitosan-based solution) to solid (two different BAG particles) ratio. The liquid phase, upon cross-linking acts as the continuous phase and the inorganic glasses as the dispersed phase, in the composite, respectively.

3.1 Materials used in preparation of cements

In the experimental part of the thesis, two cements were prepared and studied for their suitability as injectable bone substitute. Both cements consisted of a liquid and a powder phase. The liquid phase of both cements was an aqueous solution of chitosan and citric acid (distilled water as solvent). Chitosan, used in this study, was low molecular weight chitosan from Sigma Aldrich (product no. 448869) and according to the manufacturers labeling, its degree of deacetylation was more than 75%. Citric acid was also from Sigma Aldrich (product no. 251275) with purity over 99.5%. The powder phase of the composite was BAG powders with particle size less than 38 µm. In this study, two different BAGs were used: S53P4 silicate glass and calcium phosphate (PhGlass) glass. Their nominal compositions are presented in Table 3.

Table 3. *Nominal compositions of BAGs (molar ratio).*

	P_2O_5	B_2O_3	SiO_2	Na_2O	CaO	SrO	MgO
PhGlass	45.00	2.50	2.50	10.00	20.00	10.00	10.00
S53P4	1.72	-	53.85	22.66	21.77	-	-

Both glasses were prepared by the standard melt-quench method. For PhGlass, precursors used were $NaPO_3$, H_3BO_3, SiO_2, $Ca(PO_3)_2$, $SrCO_3$, NH_6PO_4 and MgO. For S53P4, precursors were SiO_2, $(CaHPO_4)\cdot 2\,H_2O$, H_3BO_3, $CaCO_3$ and Na_2CO_3. Given amounts of precursors were measured in an aluminum dish and precursors were mixed with a spoon. S53P4 was melted in platinum crucible and calcium phosphate glass in a

silica crucible in a melting oven. Melting times and temperatures can be seen in Table 4. The glasses were mixed at halfway of the melting to make sure that the resulting glass is homogeneous. After melting, glasses were poured into a graphite mold and annealed in annealing oven at composition specific temperatures and times presented in Table 4.

Table 4. *Melting and annealing parameters of BAGs*

	Melting temperature (◦C)	Melting time (h)	Annealing temperature	Annealing time
PhGlass	1000	1	425	8
S53P4	1375	1	500	8

After annealing process, glass batches were cooled down at room temperature and stored in resealable plastic bags in a desiccator cabinet until processing into powder.

3.1.1 Preparation of the chitosan solution

The chitosan solution was prepared by measuring 100 ml distilled water into a beaker. The beaker was placed on a magnetic stirrer equipped with a hot plate. Before adding the chemicals to the solution, the hot plate was adjusted to ~ 22 °C and stirring set to 600 RPM. 20 g of citric acid was then dissolved into the distilled water and stirred until all the citric acid was dissolved. Successively, 2 g of chitosan powder was diluted in the acidic solution under stirring until it was visually entirely dissolved. The beaker was covered with parafilm during the dissolution process, to avoid evaporation and contamination. The solution was always stored in a refrigerator at 6 °C when not in use.

3.1.2 Preparation of BAG powders

BAG powders were prepared from melted glass batches. BAG blocks were broken into smaller particles with a hammer. Smaller glass particles with diameter of approximately <3 mm were collected. Particles were further processed into fine powder with Fritsch Pulverisette 7 -planetary micro milling device. Particles of desired size were separated using a Retsch AS200 Sieve Shaker -sieving device. Particle size used in this study was <38 mm. BAG powders were stored in a desiccator cabinet, in labelled plastic containers, when not in use.

3.1.3 Preparation of cements

BAG/Chitosan cements were prepared by mixing the solid (BAG powder) and liquid phases (chitosan-solution) together, manually, in a glass container, with a spatula, until the mix formed a homogenous paste-like consistency. Before mixing, the chitosan solution was heated to RT, at which the preparation process was done. The first studied cement consisted of chitosan solution (liquid) and S53P4 (solid). The other cement consisted of chitosan solution (liquid) and S53P4/PhGlass (solid), with 50 wt% of both glasses in the solid phase. Liquid-solid-ratios in the cements were adjusted by increasing the amount of liquid phase while the quantity of powder phase remained the same. Both studied cements were prepared in three different L/S-ratios, which are presented in Table 5.

Table 5. *Quantities of BAG particles and chitosan solution in bone cement samples with different L/S -ratios.*

L/S -ratio (ml/g)	BAG (g)	Chitosan-solution (ml)
0.5	2	1
0.75	2	1.5
1.0	2	2

3.2 Injectability testing

In this thesis work, the injectability of the studied cements were evaluated in two different ways. Firstly, cements were prepared with different L/S-ratios and injectability were measured, by pressing the cement out of a syringe, by hand. The aim of this first phase was to find the most suitable L/S-ratio for cements, creating a smooth, homogenous, and easily injectable paste with adequate setting time.

Injectability of the prepared composite cements were investigated using 2 ml disposable injection syringes. Injectability of the cements for all L/S -ratios presented in Table 5 was tested as a function of setting time, at 5 min intervals. Testing was stopped when the cement could not be extruded out of the nozzle of the syringe in a continuous manner. Injectability was calculated as shown in equation 1:

$$Inj\% = \frac{Cement\ weight\ injected\ from\ the\ syringe}{Total\ cement\ weight\ in\ the\ syringe\ before\ injection} \times 100\% \quad (1),$$

where Inj% is the percentage of injected cement from the syringe.

After the first part of the injectability tests, the most suitable L/S-ratios of both composite cements, based on their setting time and injectability, were chosen to be further investigated for their mechanical and *in vitro* dissolution properties.

In a second time, the aim was to build an injectability testing set up using a standard mechanical tester, with which it would be possible to measure injectability behavior of these cements with better repeatability, not being dependable on the persons strength in pressing the cement out of the syringe. This is presented in the next section 3.3.

3.3 Injectability test with mechanical tester

This measurement was done by following Robinson's et al. protocol "The Quantification of Injectability by Mechanical Testing" from University of Birmingham, School of Chemical Engineering (Robinson et al., 2021). The protocol consists of five phases: sample preparation, setting up the mechanical tester and creating a testing method, setting up the clamping system, running the injectability protocol and collection of the measurement data, respectively. Samples were prepared as described in section 3.1.3. Seven samples of each condition were prepared and tested with different setting times. Setting times were chosen according to supposed total setting times of each cement investigated earlier in previous phase of the experiment (3.2).

Mechanical tester (Instron ElectroPuls® E1000) was set up in compression testing mode, according to user manual. Load cell used in this measurement was 1 kN. The height of the crosshead was adjusted so that there were enough room for the syringe and its plunger underneath the crosshead. Testing method was created in testing software, the parameters of which are presented in Table 6.

Table 6. *Testing parameters*

Parameter	Value
Test-type	Uniaxial compression
Pre-load	0.5 N
Speed to pre-load	5 mm/min
Test speed	0.5 mm/s
Upper force limit	200 N

Clamping system (Figure 11) was built by equipping two stands with clamps with large enough grips to properly hold the syringe. The clamping system should withstand relatively high downward force without collapsing. Grips were placed between the crosshead and the baseplate with enough space for the syringe and its plunger in a way that the center of the crosshead and grips were aligned with each other to achieve high quality data. Additionally, a petri dish was placed onto the bottom plate to collect the cement injected from the syringe.

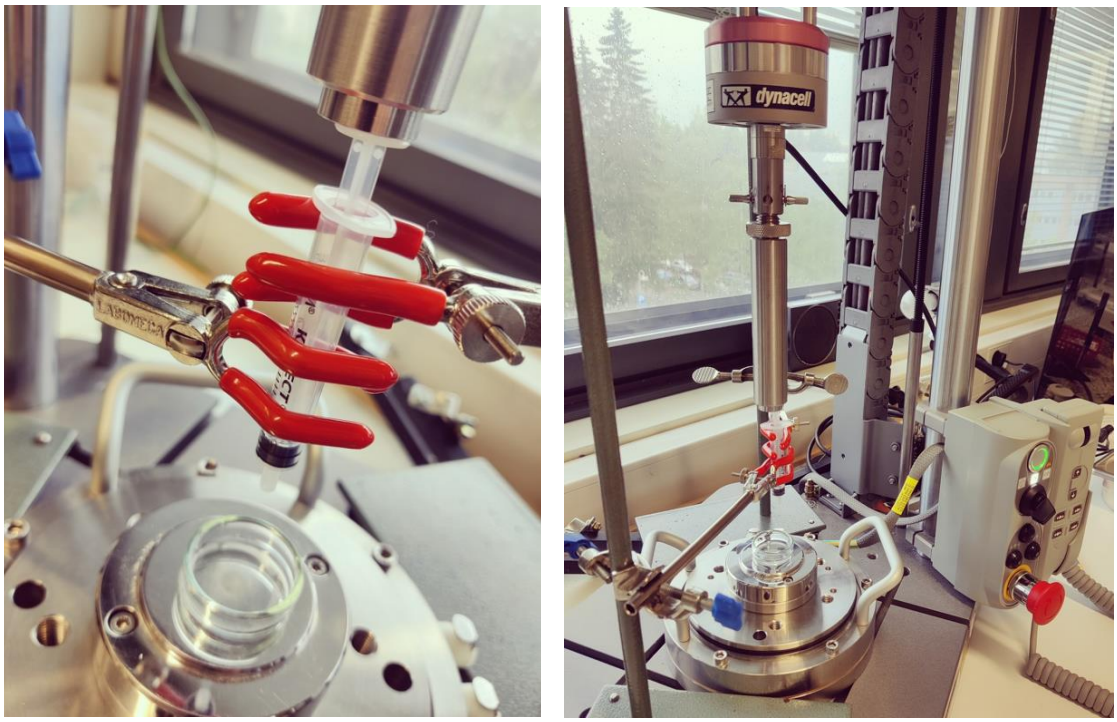

Figure 11. *Injectability testing set-up with standard mechanical tester. Cross-head presses the syringe inserted between two clamp grips.*

The actual measurement was done by inserting the syringe into the grips of the clamping system so that the syringe and its plunger were perpendicular to the crosshead and grips were holding them still without creating any resistance to the extrusion process. The

crosshead was lowered manually as close to the plunger as possible without touching it and the measurement was done by starting the created method from the measurement software. After measuring all the samples, the data were collected and plotted to get information about the change in injectability behavior with respect to the setting times.

3.4 Compression test

Compressive strength of the cements was evaluated by doing simple compression tests with the same mechanical testing device which was used in to study the injectability behavior, Instron ElectroPuls® E1000, using a 1 kN load cell. Samples were prepared following the process described in section 3.1.3. The cements were then placed inside 2 ml injection syringes and let to dry overnight. The cylindrical samples were 8 mm in diameter (diameter of the 2 ml syringe) and 9.4 ± 2.8 mm of height. Height of the samples was difficult to control in preparation phase, so every sample was measured individually. The exact dimensions of each sample were inserted in the measurement software before starting the test.

The compression test was carried out by inserting the sample in upright position onto the bottom plate of the mechanical tester and compressing the sample at a crosshead speed of 0.5 mm/min, until the sample was totally broken, or displacement reached 60 % (end of test parameter) of total sample height. From the stress-strain curve obtained, Young's modulus and stress at fracture can be defined, as shown in Figure 12 (Fjær et al., 2021):

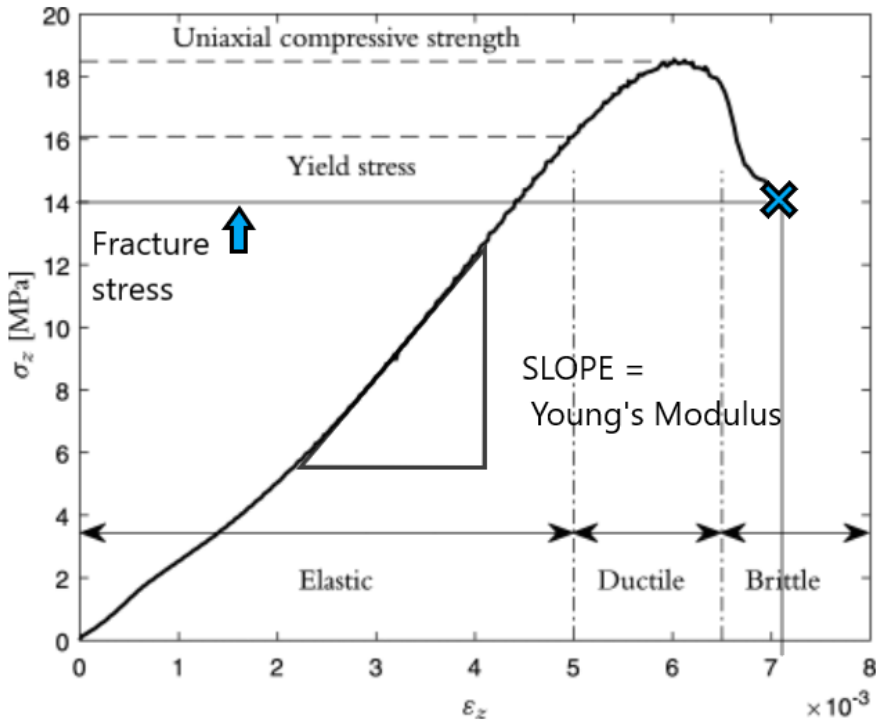

Figure 12. *Schematic picture of stress-strain curve in uniaxial compression test. Modified from (Fjær et al., 2021).*

From the compression test data, Young's modulus can be calculated as the slope of the stress-strain curve in the elastic region (Figure 12). The stress at fracture is simply the stress at which the material fails by fracture.

3.5 *In vitro* dissolution testing

The *in vitro* dissolution behavior of the studied cements was evaluated by immersing them into simulated body fluid (SBF), which is a solution mimicking the inorganic concentration in the blood plasma. SBF is used to assess bioactivity of biomaterials. Samples were let to dry inside a 2 ml syringe for 24h under a hood, prior to immersion. Mass loss of the cement, pH change and ions released in the SBF were investigated. The aim of the dissolution testing was to evaluate the degradation rates of the cements and precipitation of reactive layer at the cement surface.

3.5.1 SBF immersion

The SBF solution was prepared following the protocol described by Kokubo et al. (Kokubo et al., 1991). The reagents used are listed in Table 7. The reagents were dissolved in 1 liter of distilled water in a plastic beaker under constant stirring, in the order they are reported in Table 7. Finally, the SBF solution was heated in a hot water bath

and the pH of the solution was adjusted to 7.40 ± 0.2 at (37 ±0.2) °C with 1M hydrochloric acid (HCl). The SBF dissolution test was carried out by immersing each BAG cylinder in the SBF solution, in plastic container, and incubated in a shaking incubator at 37 °C at 100 RPM for 0 h, 6 h, 24 h, 72 h and 1 week. All time points were done in triplicates. The amount of SBF solution used in this experiment was calculated individually for each sample and the used ratio was 50 ml of SBF per 1 g of sample, thus maintaining the mass of sample to volume of SBF constant. For each time point a blank SBF (40 ml of solution without any cement sample) was incubated under the same conditions as a control. This was done to ensure the stability of the SBF over the testing period.

Table 7. *Dissolution order and amounts of precursors for SBF preparation.*

Order no.	Precursor	Amount/ 1 liter of SBF
1	NaCl	7.996 g
2	$NaHCO_3$	0.350 g
3	KCl	0.224 g
4	$K_2HPO_4 \cdot 3H_2O$	0.228 g
5	$MgCl_2 \cdot 6H_2O$	0.305 g
6	1M-HCl	40 ml
7	$CaCl_2 \cdot 2H_2O$	0.368 g
8	Na_2SO_4	0.071 g
9	$(CH_2OH)_3CNH_2$ (Trizma® Base)	6.057 g

After samples had been in SBF immersion for desired time periods, they were removed from the solution, rinsed in ethanol, and dried under hood. After drying, samples were weighed again to determine the mass loss during immersion in SBF. Mass loss of the cement samples was calculated with the following equation:

$$Mass\ loss\ (\%) = \frac{m_a - m_b}{m_a} \times 100\% \qquad (2),$$

where m_a is the initial sample mass, and m_b the sample mass after immersion in SBF.

The results were presented as average remaining mass (100 % - mass loss-%) ± standard deviation (SD) from the triplicates at each studied time point. Finally, the

samples were placed into a multi-well plate and stored in a desiccator cabinet at room temperature before further measurements.

Lastly, both the pH of the sample solutions and controls were measured at (37 ± 0.2) °C, with Mettler Toledo Seven Multi -pH meter. The results are presented as average pH (mean) ± standard deviation (SD) from the triplicates at each studied time point. After pH measurements, 1 ml of each sample and control solution was pipetted into an Eppendorf tubes and stored in freezer before further investigation.

3.5.2 ICP-OES

Both control and sample solutions were characterized by inductively coupled plasma – optical emission spectrometry (Agilent Technologies, 5110 ICP-OES). The purpose of this phase of the experiment was to evaluate ion concentrations of interest inside the solutions. Thus, the immersion solutions were defrosted and 1 ml of them were pipetted and diluted in 9 ml of 1 M HNO_3 to be characterized by ICP-OES. Table 8 presents the evaluated elements and their relative wavelengths that were used for quantification in the measurement.

Table 8. *Elements of interest in the ICP-OES measurements and their relative wavelengths.*

Element	Wavelength (nm)
B	249.772
Ca	422.673
Mg	285.213
P	213.618
Si	251.432
Sr	407.771

In this part of the experiment, three samples of each condition were evaluated per immersion time point, as well as three control samples (blank SBF). The results were presented as average concentration (mean) of each element ± standard deviation (SD) between the triplicates, at each studied time point. Mean and standard deviation were calculated from the ICP data with corresponding methods in Microsoft Excel.

3.5.3 Scanning Electron Microscopy

Cylindrical cement samples of both conditions were analyzed by Scanning Electron Microscopy (SEM) and energy-dispersive spectrometry (EDX) at Microscopy center of Tampere University. The samples evaluated in this part of the work were cements of both conditions with immersion time points of t = 0 and t = 1 week. SEM-EDX observations and analysis were made from top and cross sections of each sample to investigate the dispersion of BAG particles in the chitosan and to see how the bioactive reactive layer is forming onto the surface of the cement. Top section images were taken from the surface of the cylindrical samples. For cross section imaging, the samples were cut in half vertically with a surgical knife.

4. RESULTS & DISCUSSION

In this chapter, the results of the experimental part of the thesis are presented. Based on the results, both conditions under investigation are evaluated and discussed by their suitability to be used in IBS systems. Additionally, limitations of used methods are evaluated and required further studies are suggested.

4.1 Injectability testing by hand

The initial aim of this thesis was to evaluate both glasses separately in injectable bone cements. At the early stage of this study, it was discovered that it was impossible to get desired paste-like consistency by mixing only <38 µm PhGlass particles and chitosan solution together. The PhGlass/Chitosan cement did set almost immediately after mixing and could not be extruded out of the syringe with L/S -ratios in range of 0.5-3.0 ml/g. With higher L/S-ratios, only liquid was extruded from the nozzle of the syringe, leaving the PhGlass particles inside the syringe. Thus, the second studied cement composition was modified by mixing 50 wt-% of S53P4 glass particles with 50wt% of PhGlass, as the solid phase.

Injectability testing by hand was started with a L/S -ratio of 0.5 ml/g for both conditions and the ratio was increased by 0.25 ml/g gradually, until setting of the cement occurred in the syringe approximately 1 hour after cement preparation. To begin with, it is important to note that this testing method has some limitations with respect to repeatability. The amount of cement extruded out of the syringe is highly dependable on the person's individual force pressing the plunger and the results may vary significantly depending on the person carrying out the test. In addition, viscous nature of the chitosan solution might cause some inaccuracy in measuring the solution, because small amounts of solution might stay in the nozzle of the syringe/pipette that is used in measuring the solution. Also, small quantity of BAG particles might stick onto the walls of the glass container which can possibly cause inaccuracy compared to the theoretical L/S -ratios of the cements. It would have been beneficial to assess the inorganic content by differential thermal analysis (DTA). The same cement preparation technique is used throughout this study, so these inaccuracies are present in all parts of this thesis work. Nevertheless, the used cement preparation method is appropriate in this kind of early-

stage study, it is fast and easy to do in large quantity and enable to carry out the research using ordinary laboratory equipment in an economically effective manner.

Figure 13 presents results of injectability testing by hand for S53P4/Chitosan -cement. It shows the injectability percentage of cements as a function of setting time. In case of S53P4/Chitosan -cement, at the lowest L/S-ratio of 0.5 ml/g, no cement could be extruded out of the nozzle of the syringe, right away after preparation and weighing the syringe with the cement. This seemed to not only occur due to setting, but also filter-pressing phenomenon was observed in injection, which was also mentioned in Song's et. al. study article. This phenomenon means that the BAG particles are building up to the tip of the nozzle and only liquid is filtering through the syringe, leaving the majority of the BAG particles inside the syringe (Song et. al., 2008).

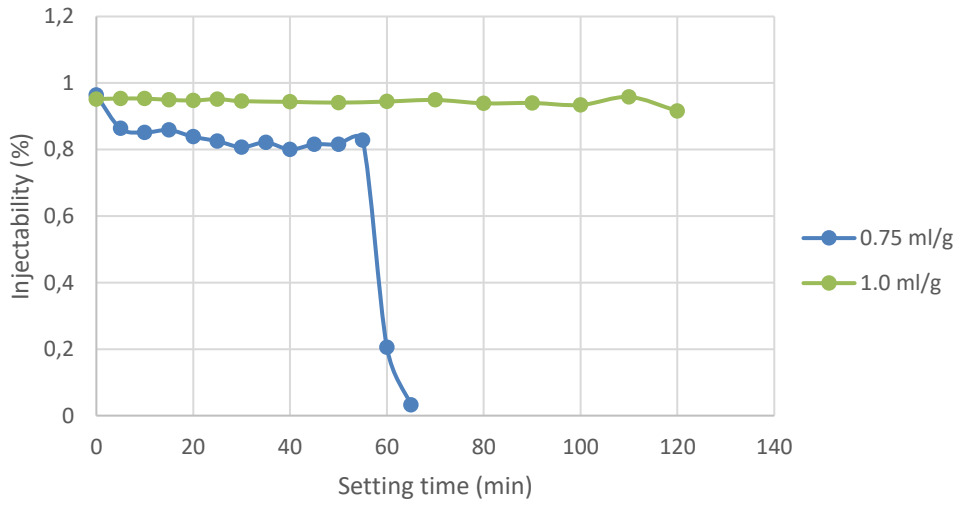

Figure 13. *Injectability behavior of S53P4/Chitosan -cement as a function of setting time.*

As can be seen in Figure 13 , after increasing the L/S -ratio to 0.75 ml/g, setting behavior changed significantly and the S53P4/Chitosan -cement was smoothly extruded from the syringe until about 50 minutes of setting, after which it started to harden inside the syringe and the injectability percentage (Inj%) dropped steeply. With 0.75 ml/g, the cement was also easily mixed into homogenous paste, and it was easy to insert inside the syringe with a spatula. For comparison, L/S -ratio was yet increased to 1.0 ml/g and as can be seen in the plot of Figure 13, cement with this ratio did not show indications of hardening even after two hours of setting. It is important to mention that, at L/S-ratio of 1.0 ml/g, the mixture was rather liquid for the first 10 minutes. After 10 minutes the mixture had a more

paste-like consistency. Liquid consistency is not desirable in case of injectable bone substitute systems. Based on previous observations, for S53P4/Chitosan -cement, a ratio of 0.75 ml/g was chosen to be further investigated.

Figure 14 presents results of injectability testing by hand for the cement composition with both glasses. For the mixed BAG condition, S53P4/PhGlass/Chitosan -cement, the same approach was used beginning with 0.5 ml/g L/S -ratio. The graph in Figure 14 indicates, that with the lowest ratio of 0.5 ml/g, the cement started to harden in the syringe relatively fast after cement preparation, approximately 10 minutes afterwards, and the total hardening of the cement occurred very quickly resulting in a steep drop in the injectability percentage (Inj%). By increasing the L/S -ratio to 0.75 ml/g, the setting behavior and the consistency of the paste seems to change similarly to what was described for the S53P4/Chitosan -cement.

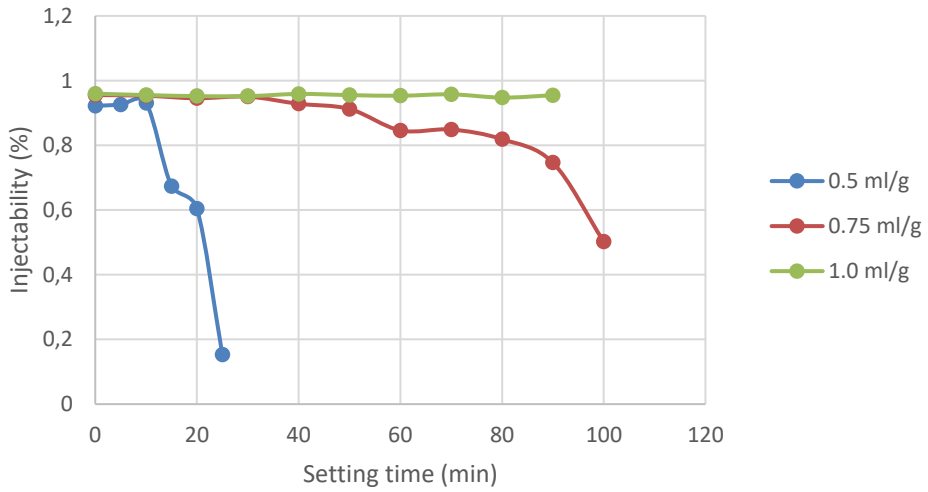

Figure 14. *Injectability behavior of S53P4/PhGlass/Chitosan -cement as a function of setting time.*

The cement was easily mixed in the glass container into homogenous paste and sample handling was easy. However, the S53P4/PhGlass/Chitosan -cement retained its paste-like consistency longer than the cement with only S53P4 without hardening in the syringe. This suggests that by mixing phosphate glass into the cement, setting time is increasing while maintaining relatively similar paste-like consistency of the cement.

Figures 15.A and 15.B are presenting the change in consistencies of the studied cements as function of setting time. The setting times are gradually increasing from t=0 to close

to total setting time where none of the paste is coming out of the nozzle of the syringe anymore. The consistency of S53P4/Chitosan -cement is looking drier, which is possibly causing cutting of the paste string at higher setting times while with the cement with mixed glasses, more continuous string of paste is extruding out of the syringe. In addition, the paste with mixed glasses seems to have more moisture on its surface compared to the one containing only S53P4.

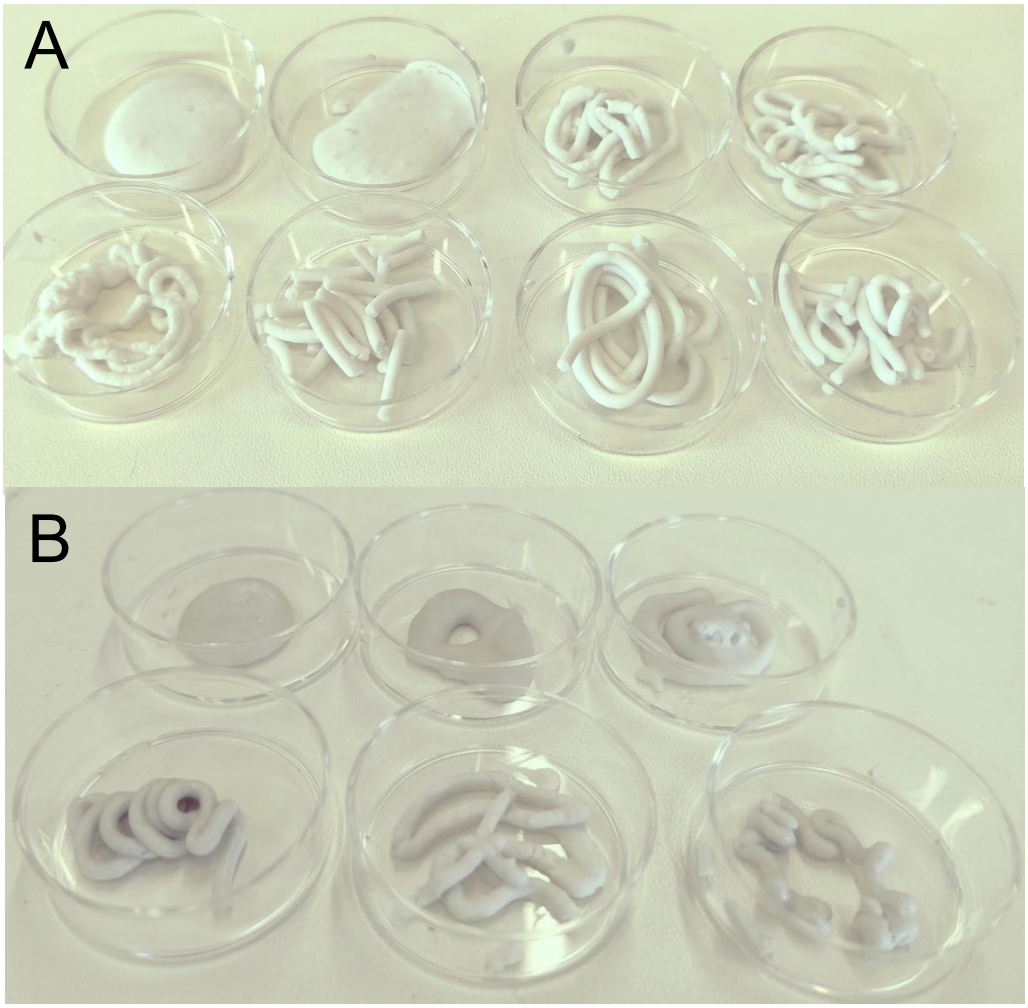

Figure 15. *Cement consistencies after extrusion from the syringe with increasing setting time. (A) = S53P4/Chitosan & (B) = S53P4/PhGlass/Chitosan.*

Compared to optimal setting times based on previous literature, these setting times achieved with the best cement consistencies are relatively slower than the optimal setting times of 15 minutes (Demir-Oğuz et. al., 2023). As a result, further investigation will be needed in future to find ways of decreasing the setting time while still maintaining the

optimal injectability behavior and consistency of these pastes, which was not possible to investigate in the scope of this thesis work.

4.2 Injectability testing protocol with mechanical tester

Injectability testing set up (Section 3.3.) was build following the Robinson's et al. protocol (Robinson et al., 2021). The goal was to achieve an applicable method of measuring the injectability of bone cements with good repeatability in laboratory circumstances using ordinary laboratory equipment and standard mechanical tester.

The set up was build succesfully and measurements were also carried out with good outcome after a few test measurements and adjustment of testing parameters. However, there occurred some limitations, which will require development in the future to get valid information about injectability of the cement samples.The results are presented in Figure 16. The figure shows the stress for strain varying between 0-20%. As can be seen in Figure 16, the stress needed to extrude the cement from the syringe was increasing gradually with longer setting times, which was also supposed to be happening before the experiment. The cement injected right away after preparation had plateau stress of 0.05 MPa, whereas the cement with setting time close to the total hardening of the cement had plateau stress of 0.4 MPa. Some variation can be seen between the cements with different setting times, as well as local rises and decreases in stresses can be observed. These were evaluated to occur due to resistance in plunger movement caused by compressive forces of the clamp grips to the syringe walls. Distinct maximum stress peaks does not occur with the tested cements, which tells that the stress needed to extrude the cement from the syringe at constant speed is greater than the stress needed to overcome friction caused by the syringe walls. This behavior is common with viscous samples going through very thin gaps. (Robinson et.al., 2020)

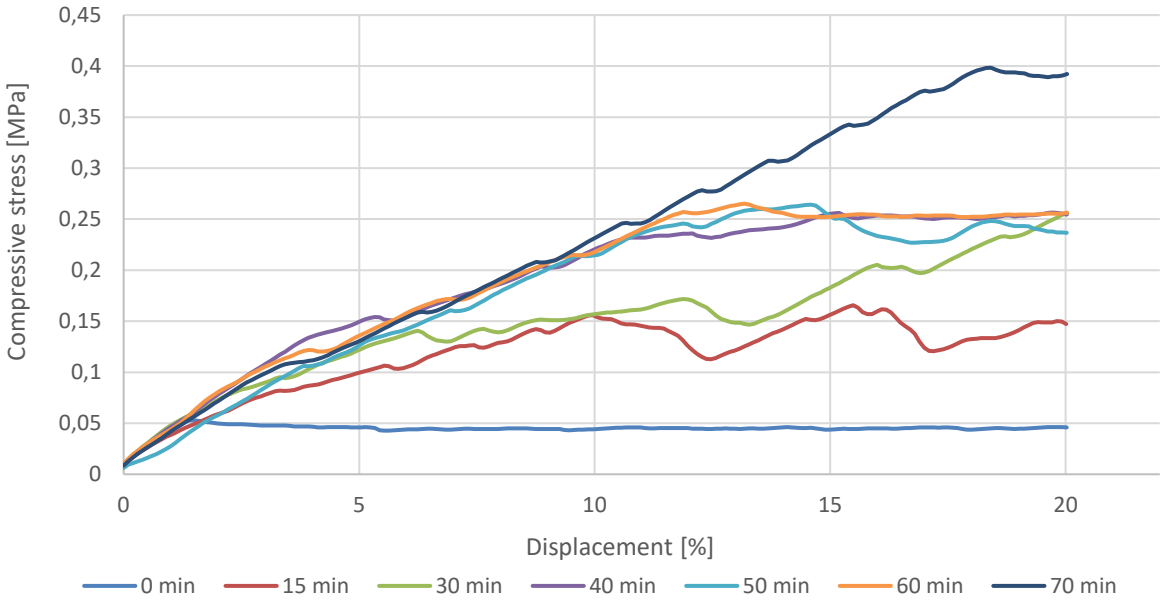

Figure 16. *Compressive stresses applied to the plunger of the syringes containing 0,75 ml/g S53P4/Chitosan -cement with different setting times in function of cross head displacement in the compression test.*

The major limitation of the set up was that the clamping system started to yield with higher stresses, which has an influence on the stress-displacement graph. The difficulty of keeping the syringe completely still during the measurement with higher forces needs to be overcome in the future by developing stronger clamping system around the mechanical tester.

4.3 Compression test

Mechanical properties of non-immersed IBS samples were evaluated by compression test with standard mechanical tester as described in section 3.4. The results of mechanical properties in compression test are presented for S53P4/Chitosan - and S53P4/PhGlass/Chitosan -cements in Tables 9 and 10, respectively. From the results, it can be said that with the cement consisting of both BAGs, better mechanical properties were achieved in general compared to the one with only S53P4 as the powder phase.

Table 9. *Mechanical properties of S53P4/Chitosan -cement in compression test.*

Sample	Diameter [mm]	Height [mm]	Young's Modulus [MPa]	Max compressive stress [MPa]	Compressive strain at max compressive stress [%]
1	8	7	71	10.0	60
2	8	6	67	10.7	53
3	8	8	64	8.2	29
4	8	7	69	10.1	41
Mean	8	7	68	9.7	46
SD	0	0.7	3	0.9	11

Table 10. *Mechanical properties of the S53P4/CaP/Chitosan -cement in compression test.*

Sample	Diameter [mm]	Height [mm]	Young's Modulus [MPa]	Max compressive stress [MPa]	Compressive strain at max compressive stress [%]
1	8	7	121	16.4	27
2	8	8	174	13.9	22
3	8	6	76	15.8	37
4	8	7	120	13.1	24
Mean	8	7	123	14.8	28
SD	0	0.7	35	1.3	6

The maximum compressive stress of both cements seems to be approximately in the upper range of compressive strength reported for the trabecular bone (Table 1.) Based on results, it can be, thus, reassured, that both cements are promising based on their mechanical properties, to be used as bone substitute materials in non-load bearing applications, especially in reconstruction of trabecular bone in case of bone voids and other smaller defects.

Even though cracks started to propagate relatively early on, in compression test, the samples held on well and could withstand increasing compressive load effectively. At the end of the test, when the maximum compressive stress was reached, the samples collapsed totally due to multiple propagated cracks during the test with increase in applied compressive stress.

4.4 *In vitro* dissolution

Figure 17 presents the results of mass loss of the cylindrical cement samples during the immersion in SBF as function of immersion time. Based on mass loss data during the immersion, both cements lost their mass relatively fast during the first couple of days of the immersion, but mass loss slowed down after about 72h. For immersion time longer than 72h almost no mass loss was recorded. The cement with only S53P4 as powder phase had about 80 % of the original mass remaining after 1 week of SBF immersion of the cement with S53P4/PhGlass had approximately 70 % of remaining mass. Furthermore, the cement with both glasses was losing its mass a little faster at the beginning of SBF immersion compared to the cement with only S53P4. These observations are suggesting that most of the calcium phosphate glass is dissolved from the cement to the solution during 1 week of immersion in SBF solution. This is coherent with the typically faster dissolution rate of metaphosphate glasses compared to the silicate bioactive glasses. However, this will be further evaluated based on ICP results. It is also noteworthy that the mass loss, in bioactive materials is not straightforward. Indeed, it is assumed that the simultaneous precipitation of the reactive layer also effect on mass change. While dissolution leads to mass loss, the precipitation of the reactive layer would lead to mass gain.

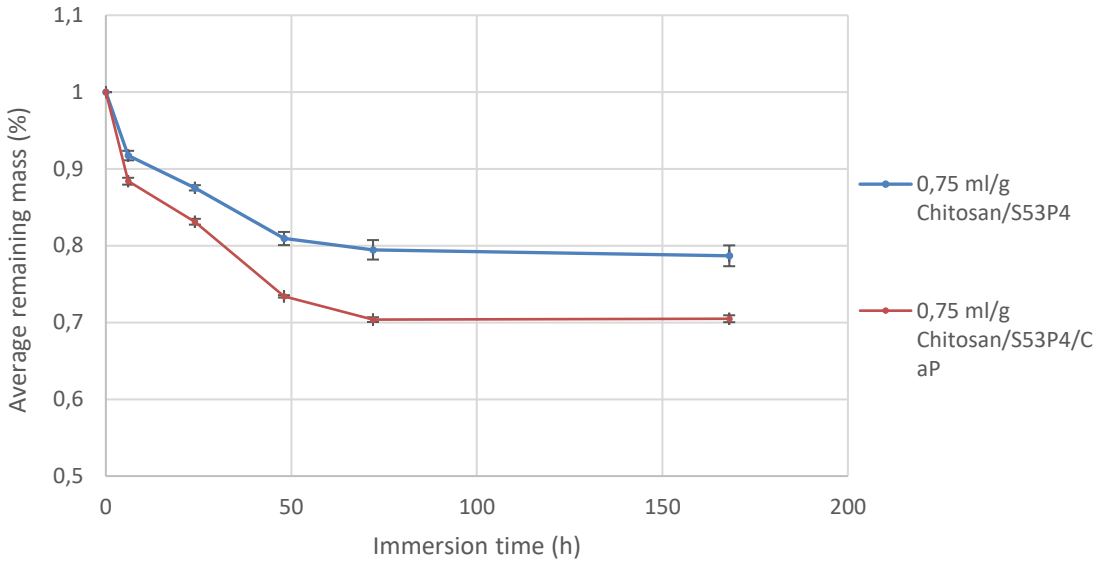

Figure 17. *Mass loss of both cements during immersion in SBF solution*

Figure 18 presents the pH change in the SBF during sample immersion. It shows that dissolution of the cement with mixed glasses is causing a slight drop in pH of the SBF to approximately 7.0. On the contrary, dissolution of the S53P4 -cement is increasing the pH of SBF to approximately 8.4 during immersion, which can be assumed to occur due to basic nature of the silica dissolution products. The pH of the blank SBF sample is not changing significantly during the 1 week incubation period, which tells that SBF remained relatively stable over the testing period, which is important to get valid test data of the sample dissolution. Increase in pH, upon immersion of silicate bioactive glasses, is a phenomenom well documented. The rise in pH is associated with the release of the alkaline and alkaline earth ions and consumption of H^+, from the solution, to form silanols (Hench, 1998; Nandi et al., 2011).

While silicate dissolution leads to an increase, the dissolution of metaphosphate glasses is usually associated with a slight decrease in pH, due to the high phosphorus release (Gao et.al., 2000; Li et.al., 2021). The greater mass loss, along with decrease in pH of the cements containing the two glass composition tend to indicate a faster dissolution rate of the phosphate phase.

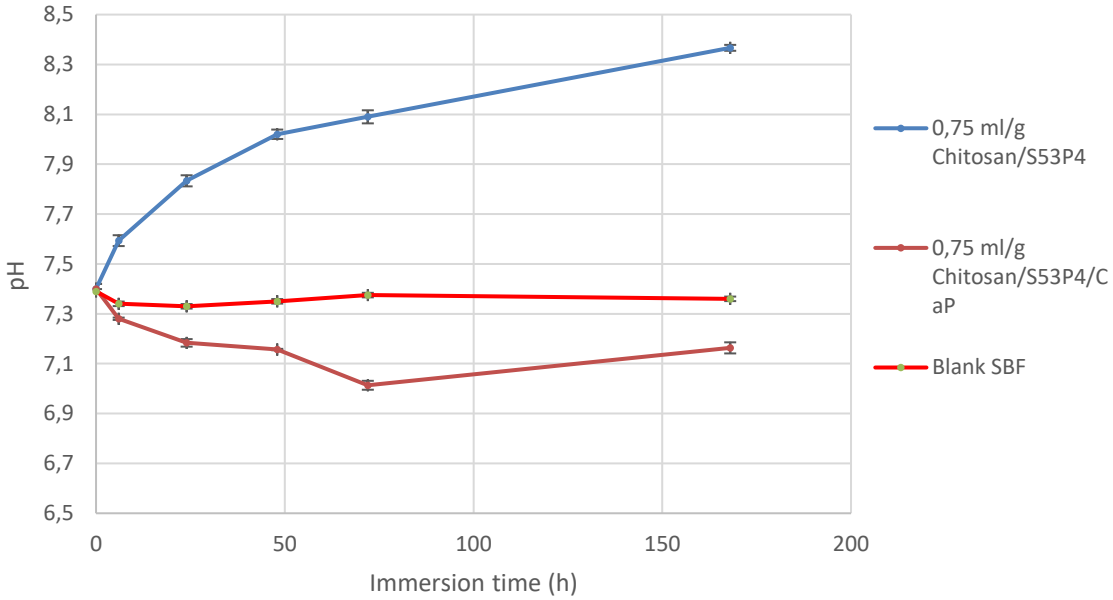

Figure 18. *pH change of the SBF solution during immersion.*

Figure 19 presents silicon (A) and boron (B) concentrations in the SBF, during sample immersion, for both cements and the blank SBF. Si and B are glass formers, so they don't interact with ions of the solution, which means that dissolution of inorganic content of the cements can be seen from these concentrations. Figure 19.A indicates, that in the beginning of immersion for both cements, silicon concentrations start to increase rapidly, followed by a decrease for S53P4-cement. The increase is slowing down also in case of S53P4/PhGlass -cement. As expected, the release of Si is initially fast and then slows down due to the silica rich layer polycondensation. The slight decrease in Si in the solution containing the S53P4 glass containing cements is either due to an experimental error or, possibly, interaction between the Si and the chitosan. The lower release in Si from the S53P4/PhGlass composite is most likely only due to the lower overall Si available in the cement. As can be seen in Figure 19.A, also high concentration of boron is released from the PhGlass from the cement with mixed glasses, which needs to be taken into consideration in the future, because high concentrations of boron can potentially be toxic to cells, decreasing proliferation and cell viability (Ying et al., 2011). Despite the low boron content in the PhGlass composition, the high boron concentration may indicate almost full dissolution of the phosphate glass.

Figure 20 presents phosphorus (A) and calcium (B) concentrations of the SBF during sample immersion. Figure 20.A shows that PhGlass containing cement releases very

high concentration of phosphorus, which explains the pH decrease observed in pH measurements. This occurs due to phosphorus binding to OH- ions from the solution, resulting in phosphoric acid (H_3PO_4) (National Center for Biotechnology Information, 2024). Too high release of phosphorus can also be toxic to cells, which is why it needs to be studied more in the future. During the dissolution, increase of the phosphorus concentration slows down and reaches plateau, which can be interpreted as phosphorus consumption to formation of the reactive layer. As seen in Figure 20.B, calcium concentrations in SBF with both cements seems to increase in the beginning, after which their release slows down, which can be supposed to occur due to calcium consumption in precipitation of the reactive apatite layer.

Figure 21 presents strontium (A) and magnesium (B) concentrations of the SBF during sample immersion. Figure 21.A shows that PhGlass containing cement releases strontium to the solution with increasing rate at first, followed by a drop in the concentration. This observation leads to supposition of strontium being partially integrated in the reactive layer (Massera et al., 2013). Some of the Sr ions remains in the solution, which is known to provide therapeutic effects for bone healing (Marie et al., 2001). Lastly, Figure 21.B shows, that the cements are not releasing significant amount of magnesium inside the solution, as the Mg concentration of the blank sample is following the same concentration profile as the cement samples. Also in this case, Mg concentration is starting to decrease at longer immersion time, which again suggests that also magnesium is integrated in the precipitation of the reactive layer.

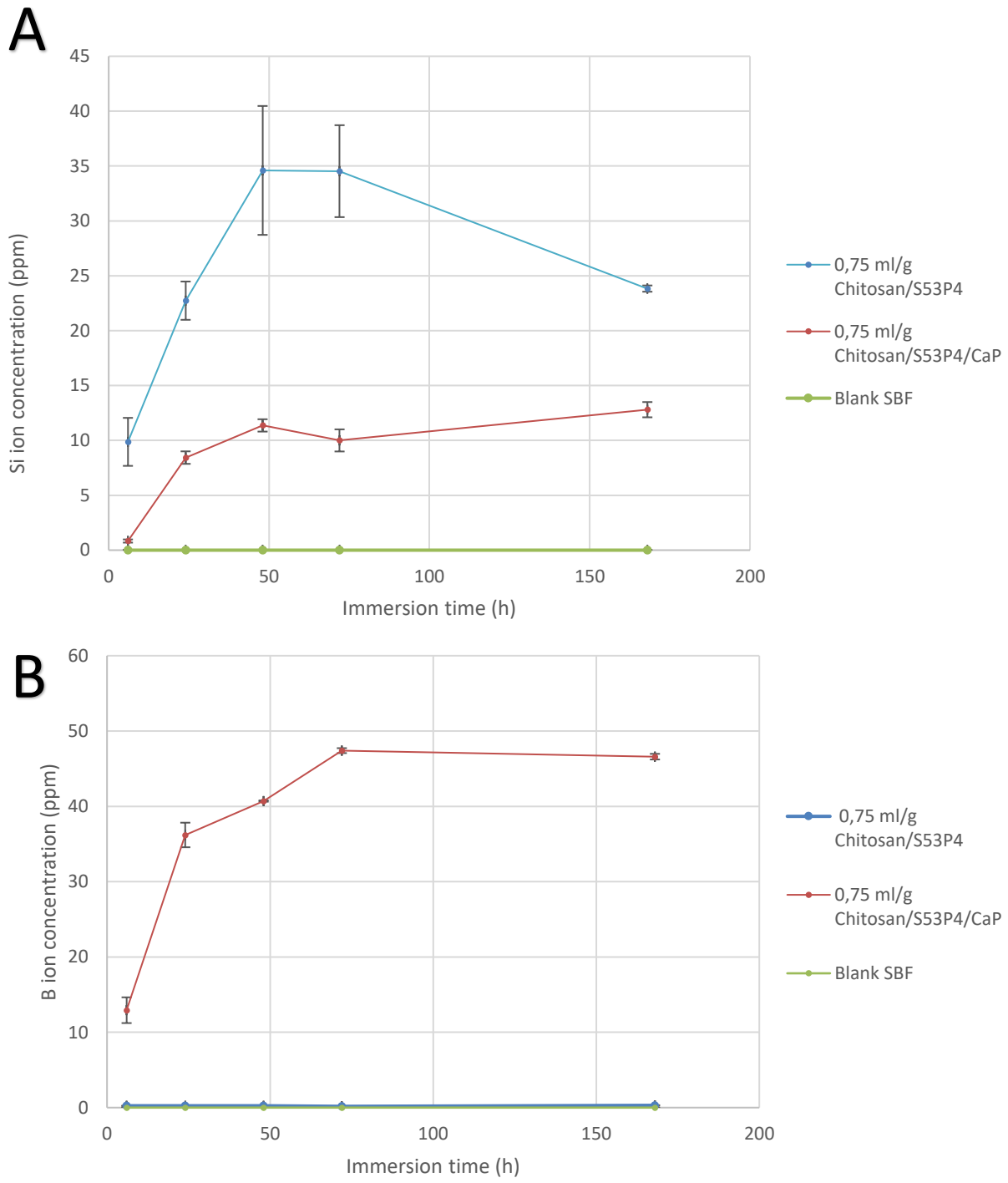

Figure 19. *Change of silicon (A) and boron (B) concentration in SBF during immersion.*

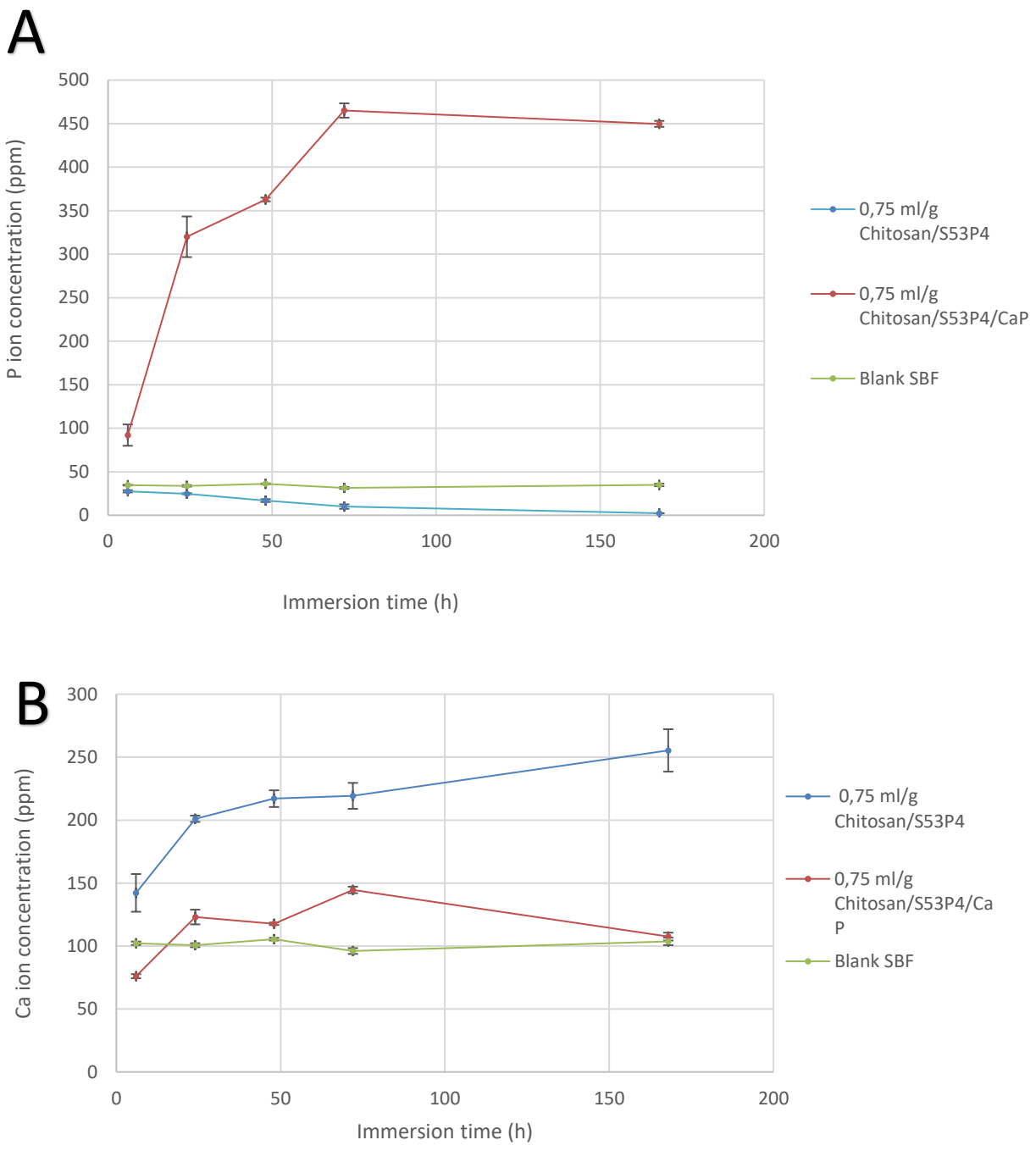

Figure 20. *Changes in phosphorus (A) and calcium (B) concentrations in SBF during immersion.*

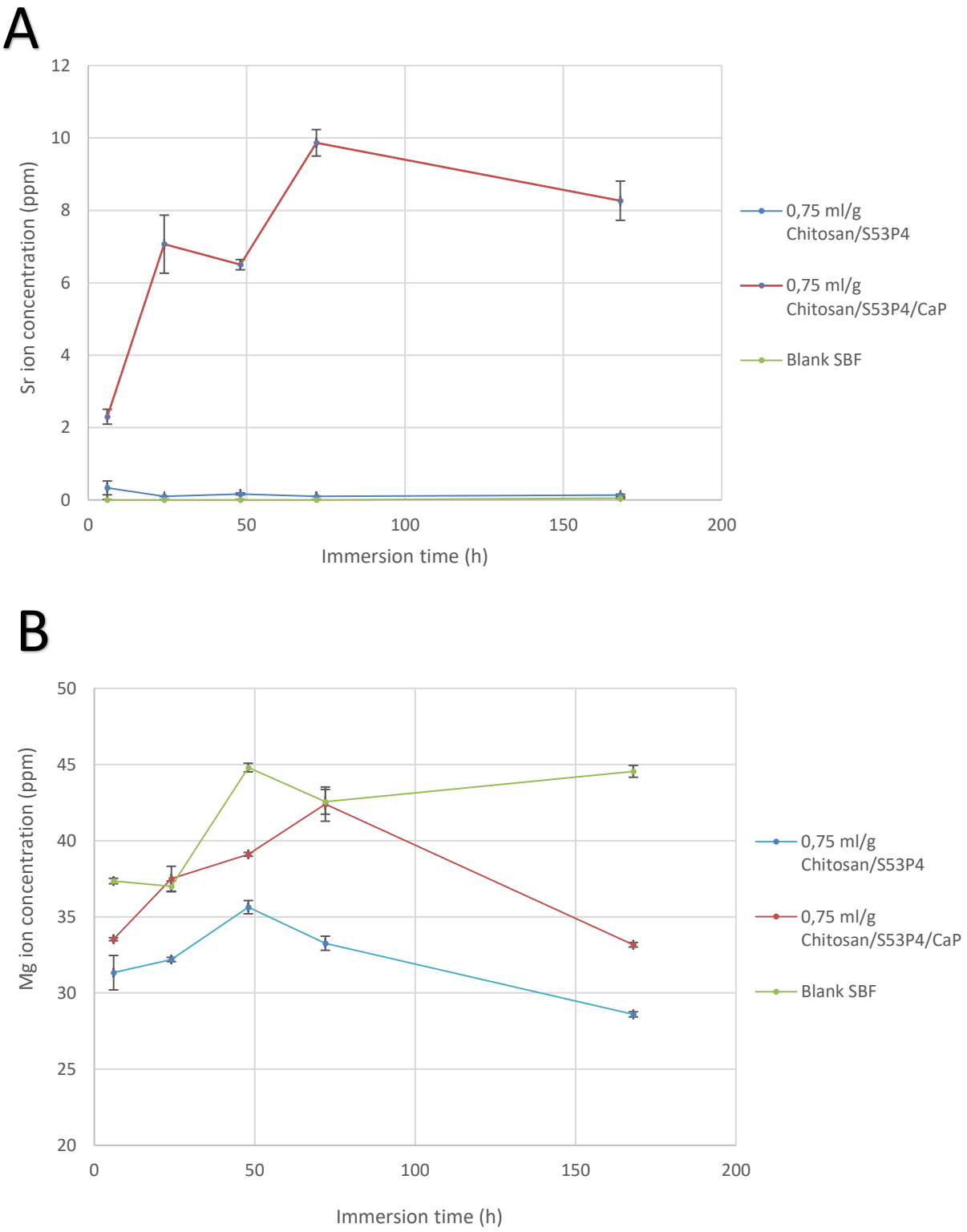

Figure 21. *Changes in (A) strontium and (B) magnesium concentrations in SBF during immersion.*

As conclusion, based on concentrations of dissolved ions in SBF, it seems that both S53P4 and PhGlass are degrading from the cements, which means that the chitosan allows them to dissolve from the structure of cement. Also, mass loss data suggested fast dissolution of the PhGlass further confirmed by ICP data. Additionally, results are indicating precipitation of reactive apatite layer on both cements during SBF immersion, but this observation needs to be yet proven by SEM-EDX analysis.

4.5 SEM

Figure 22 presents the cross- and top-section images of the S53P4/Chitosan cement taken by SEM, after 1 week of immersion in SBF. It shows indications of reactive layer precipitation on the surface as well as inside the cement samples. The reactive HA-like layer can be seen in Figure 22 and can be recognized from SEM images by its “cauliflower-like” 3D-structure.

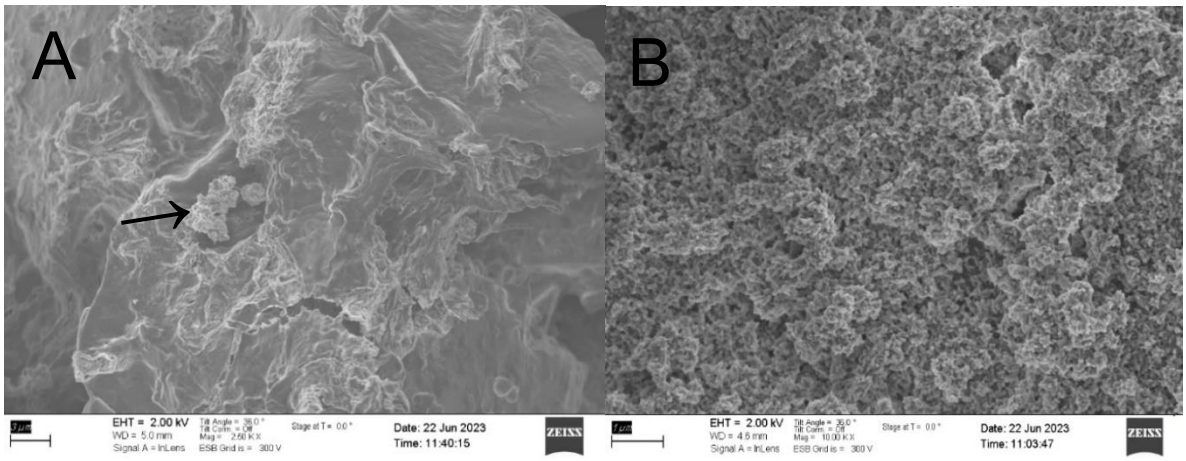

Figure 22. *Indications of reactive apatite layer precipitation in S53P4/Chitosan cement: (A) cross-section (arrow indicating formed apatite) and (B) top section in SEM.*

Figure 23 presents the cross section image of the cement with mixed glasses after 1 week of SBF immersion. SEM-EDX shows that reactive layer integrated by Mg and Sr is precipitated on the surface of the IBS after one week of immersion in SBF. This confirms the observation that was made based on results of ICP evaluation earlier. Based on EDX analysis, the reactive layer precipitating on the surface is supposed to be a layer of dicalcium phosphate dihydrate ($(CaHPO_4) \cdot 2H_2O$) integrated by Mg and Sr as suggested before.

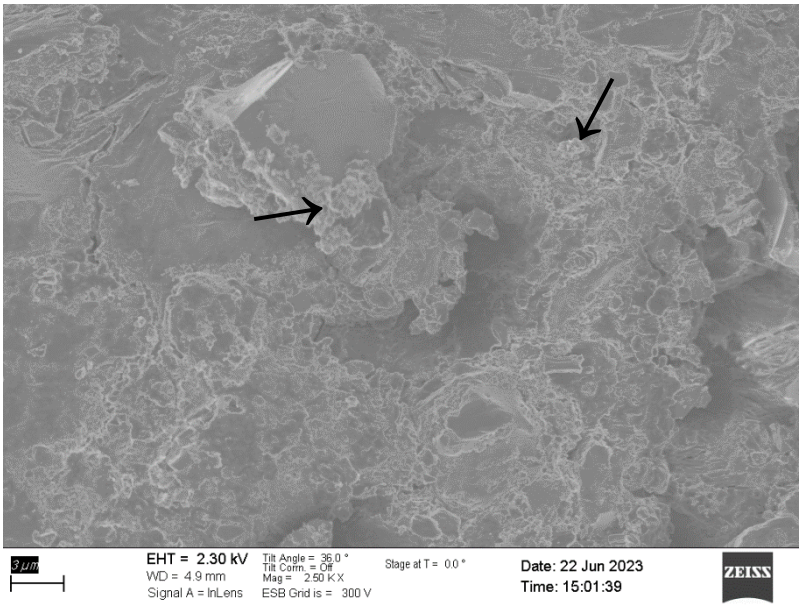

Figure 23. *Indications of reactive layer precipitation in cross-section image of S53P4/PhGlass -cement after 1 week of SBF immersion.*

With the other condition, the cement consisting of only S53P4 as the powder phase, indications of the precipitation of reactive apatite layer can be seen in some SEM images (Figure 22), but the EDX analysis is inconclusive compared to the observations in the SEM images. Since the EDX analysis does not confirm the precipitation of reactive apatite layer which could be seen in some SEM images, the condition with only S53P4 needs further investigation in the future to make sure that the reactive layer precipitates and provides bioactive properties to the IBS, enabling the bone bonding ability. It is possible that the reactive layer is thin and sparsely dispersed at the surface, leading to innacuracies in the EDX analysis.

However, cross sections of SEM images showed that the structure of both conditions had allowed the SBF solution to penetrate inside the cement and started to react also with the inner volume of the cement. This suggests that the cements manufactured, ensures the water and nutrient supply through the whole structure.

5. CONCLUSIONS

In this thesis work, two different formulations of injectable composite bone cements consisting of S53P4 silicate and calcium phosphate bioactive glasses as powder phase and gel-like aqueous solution of 2 wt-% chitosan and 20 wt-% citric acid as liquid phase. First condition was a cement with only S53P4 as powder phase and the second was a cement with both S53P4 and PhGlass with ratio of 50/50.

In the first phase of the experimental part, injectability of both conditions were evaluated by extruding cements through a 2 ml injection syringe with different L/S -ratios, as a function of setting time. Additionally, the best L/S – ratios were chosen for both conditions to be further studied in the next phases of the laboratory experiments. Secondly, *in vitro* dissolution of the cements was studied by preparing SBF solution and immersing the samples for 1 week in it. Mass loss of the samples and change in pH of the SBF solution were evaluated at 5 different time points and additionally, concentrations of dissolved ions of interest were studied by ICP-OES measurements. ICP-OES tend to indicate that the phosphate glass dissolves faster than the silicate glass. ICP-OES also suggests precipitation of a reactive layer. Lastly, SEM-EDX analysis were done at the cross- and top sections of non-immersed samples and samples that were immersed for 1 week in SBF. Based on ICP-OES and SEM-EDX results, the reactive apatite layer formation onto the cement samples was confirmed.

In the injectability test by hand it was noticed that filter-pressing phenomenon occurred on both conditions at L/S ratios lower than 0.5 ml/g. This means that BAG particles are causing clots at the tip of the syringe, and only some of the liquid phase can filter through the syringe. By increasing the L/S -ratio to 0.75 ml/g in case of both cements, homogenous and smooth pastes were achieved with good injectability, but the setting times were relatively high compared to those found from the literature, with setting time of approximately 15 minutes. Too long setting time increases the risk of cement wash out, which might result in bloggakes in blood stream. Thus, decreasing the setting times while retaining good injectability will require further studies in the future. Both cements with 0.75 ml/g were chosen to be further studied in the next phases of the experiment.

Additionally, an injectability testing set up with higher repeatability using standard mechanical testing device was built according to a protocol found from the literature. In scope of this thesis work, the aim was to build, execute test measurements, and evaluate possible limitations of the method in order to develop it to be used in the future, for the

measuring the injectability of bone cements and other injectable materials/substances. The setup was build succesfully with a few limitations, considering the resistance of the clamp grips.

In compression test, the S53P4/PhGlass -cement showed higher mechanical properties compared to the cement with just S53P4 as powder phase. Compressive strains at maximum stresses of S53P4/PhGlass and S53P4 -cements were approximately 24% and 46%, respectively. However, both cements showed good withstanding of compressive stress, even though cracks started to propagate in both samples at early stage of the test. Based on compression test, both cements are suitable by their mechanical properties to support defected bone during the healing process.

SBF immersion test indicated, that the S53P4/PhGlass -cement was losing its mass faster than the S53P4 -cement, which suggested that most of the PhGlass had dissolved into the SBF during 1 week of immersion. This could be confirmed by ICP, showing that high release of phosphorus was occurring from the S53P4/PhGlass, decreasing the pH. This was also noticed in pH measurements. Too low pH is toxic to cells, so too high phosphorus release will be considered in the future. Additionally, S53P4/PhGlass -cement was releasing relatively high concentrations of boron, which might inhibit cellular viability. However, ICP indicated formation of reactive apatite layer integrated with Sr and Mg ions, which could be confirmed by SEM-EDX analysis. In case of S53P4, ICP results also suggested formation of reactive apatite layer and even though some SEM images were showing indications of HA like layer on the surfae of the cement, EDX analysis was inconclusive and couldn’t confirm what could be seen in SEM images. Thus, reactive layer formation needs more studying at least in case of S53P4 to make sure that the formation of apatite layer is actually occuring. Nevertheless, SEM images gave promising information of both cements, because indications of reactive layer formation could be seen both on the surface and inside the cylindrical samples.

As a conclusion, both studied cements showed promising performance to be used in IBS applications, but further investigation is needed in the future considering setting times and limiting release of possibly toxic concentrations of ions during dissolution in SBF. Additionally, it is important to confirm that the reactive apatite layer is forming properly on the surface of the biomaterial, giving the cement optimal bioactivity for the application.

SOURCES

Bianco, Alessandra., Cacciotti, Ilaria., & Cappelloni, Ilaria. (2013). Bone and biomaterials for bone tissue engineering. Trans Tech Publications.
Biocomposites: Recent Advances. (2023). IntechOpen. https://doi.org/10.5772/intechopen.104003

Biogennix. (2021). Bone Fracture Repair Anatomy: 3 Ways to Categorize Bone. Bone Healing. https://biogennix.com/bone-healing/bone-anatomy-bone-fracture-repair-3-ways-to-categorize-bone/

Bloise, N., Bloise, N., & Fassina, L. (2015). Biomaterials for Bone Tissue Engineering 2020. MDPI - Multidisciplinary Digital Publishing Institute.

Brauer, D. S. (2015). Bioactive Glasses-Structure and Properties. Angewandte Chemie (International ed.), 54(14), 4160–4181. https://doi.org/10.1002/anie.201405310

Brow, R. K. (2000). Review: The structure of simple phosphate glasses. Journal of non-crystalline solids, 263, 1–28. https://doi.org/10.1016/S0022-3093(99)00620-1

Cailleteau, C., Weigel, C., Ledieu, A., Barboux, P., & Devreux, F. (2008). On the effect of glass composition in the dissolution of glasses by water. Journal of non-crystalline solids, 354(2–9), 117–123. https://doi.org/10.1016/j.jnoncrysol.2007.07.063

Costa-Pinto, A. R., Martins, A. M., Castelhano-Carlos, M. J., Correlo, V. M., Sol, P. C., Longatto-Filho, A., Battacharya, M., Reis, R. L., & Neves, N. M. (2014). In vitro degradation and in vivo biocompatibility of chitosan–poly(butylene succinate) fiber mesh scaffolds. Journal of bioactive and compatible polymers, 29(2), 137–151. https://doi.org/10.1177/0883911514521919

Currey, J. D. (2013). Bones: Structure and Mechanics. Princeton University Press. https://doi.org/10.1515/9781400849505

Davim, J. Paulo. (2014). Biomedical composites: Materials, manufacturing and engineering. Walter de Gruyter GmbH & Co., KG. https://doi.org/10.1515/9783110267488

Demir-Oğuz, Ö., Boccaccini, A. R., & Loca, D. (2023). Injectable bone cements: What benefits the combination of calcium phosphates and bioactive glasses could bring? Bioactive materials, 19, 217–236. https://doi.org/10.1016/j.bioactmat.2022.04.007

Deshmukh, K., Kovácík, T., Kenek, T., Docheva, D., Stich, T., & Pola, J. (2020). Recent advances and future perspectives of sol-gel derived porous bioactive glasses: A review. RSC advances, 1(56), 33782–33835. https://doi.org/10.1039/d0ra04287k

Dutta, P. Kumar. (2016). Chitin and Chitosan for Regenerative Medicine (1st ed. 2016.). Springer India. https://doi.org/10.1007/978-81-322-2511-9

Faqhiri, H., Hannula, M., Kellomäki, M., & Massera, J. (2019). Effect of melt-derived bioactive glass particles on the properties of chitosan scaffolds.

Fjær, E., Holt, R. M., Horsrud, P., & Raaen, A. M. (2021). Petroleum Related Rock Mechanics (3rd edition, Vsk. 53). Elsevier Science & Technology. https://doi.org/10.1016/C2021-0-03393-9

Florencio-Silva, R., Sasso, G. R. da S., Sasso-Cerri, E., Simões, M. J., & Cerri, P. S. (2015). Biology of Bone Tissue: Structure, Function, and Factors That Influence Bone Cells. BioMed research international, 2015, 421746–17. https://doi.org/10.1155/2015/421746

Francis, R., & Kumar, D. S. (2016). Relevance of Natural Degradable Polymers in the Biomedical Field. John Wiley & Sons, Incorporated, 303-360. https://doi.org/10.1002/9783527690916.ch11

Fu, Q., Saiz, E., Rahaman, M. N., & Tomsia, A. P. (2011). Bioactive glass scaffolds for bone tissue engineering: State of the art and future perspectives. Materials Science & Engineering C, 31(7), 1245–1256. https://doi.org/10.1016/j.msec.2011.04.022

Gao, H., Tan, T., & Wang, D. (2004). Dissolution mechanism and release kinetics of phosphate controlled release glasses in aqueous medium. Journal of controlled release, 96(1), 29–36. https://doi.org/10.1016/j.jconrel.2003.12.031

Gerhardt, L.-C., & Boccaccini, A. (2010). Review – Bioactive Glass and Glass-Ceramic Scaffolds for Bone Tissue Engineering. Materials, 3. https://doi.org/10.3390/ma3073867

Ghanavati, S., Petit, L., & Massera, J. (2023). New Mg/Sr phosphate bioresorbable glass system with enhanced sintering properties.

Ghassemi, T., Shahroodi, A., Ebrahimzadeh, M. H., Mousavian, A., Movaffagh, J., & Moradi, A. (2018). Current concepts in scaffolding for bone tissue engineering. Archives of bone and joint surgery, 6(2), 90–99. https://doi.org/10.22038/abjs.2018.26340.1713

Granke, M., Does, M. D., & Nyman, J. S. (2015). The Role of Water Compartments in the Material Properties of Cortical Bone. Calcified tissue international, 97(3), 292–307. https://doi.org/10.1007/s00223-015-9977-5

Gu, H., Liu, C., Zhu, J., Gu, J., Wujcik, E. K., Shao, L., Wang, N., Wei, H., Scaffaro, R., Zhang, J., & Guo, Z. (2018). Introducing advanced composites and hybrid materials. Advanced composites and hybrid materials, 1(1), 1–5. https://doi.org/10.1007/s42114-017-0017-y

Hench, L. L. (1998). Bioceramics. Journal of the American Ceramic Society, 81(7), 1705–1728. https://doi.org/10.1111/j.1151-2916.1998.tb02540.x

Hench, L. L. (2013). An introduction to bioceramics, second edition. https://doi.org/10.1142/P884

Houaoui, A., Szczodra, A., Lallukka, M., El-Guermah, L., Agniel, R., Pauthe, E., Massera, J., & Boissiere, M. (2021). New generation of hybrid materials based on gelatin and bioactive glass particles for bone tissue regeneration.

Kaur, G. (2017). Bioactive Glasses: Potential Biomaterials for Future Therapy. Springer International Publishing. https://doi.org/10.1007/978-3-319-45716-1

Khoshakhlagh, P., Rabiee, S. M., Kiaee, G., Heidari, P., Miri, A. K., Moradi, R., Moztarzadeh, F., & Ravarian, R. (2017). Development and characterization of a bioglass/chitosan composite as an injectable bone substitute. Carbohydrate polymers, 157, 1261–1271. https://doi.org/10.1016/j.carbpol.2016.11.003

Killion, J. A., Kehoe, S., Geever, L. M., Devine, D. M., Sheehan, E., Boyd, D., & Higginbotham, C. L. (2013). Hydrogel/bioactive glass composites for bone regeneration applications: Synthesis and characterization. Materials Science & Engineering C, 33(7), 4203–4212. https://doi.org/10.1016/j.msec.2013.06.013

Kokubo, T., Hata, K., Nakamura, T., Yamamuro, T. (1991). Apatite formation on ceramics, metals and polymers induced by CaO SiO2 based glass in a simulated body fluid. Bioceramics, Proceedings of the 4th International Symposium on Ceramics in Medicine London, UK, pp. 113–120, https://doi.org/10.1016/ B978-0-7506-0269-3.50020-7.

Kucera, T., Urban, K., & Ragkou, S. (2012). Healing of cavitary bone defects. European journal of orthopaedic surgery & traumatology, 22(2), 123–128. https://doi.org/10.1007/s00590-011-0831-9

Lakshmikantha, R., R, R., Anavekar, R., & Ayachit, N. (2012). Characterization and structural studies of vanadium doped lithium–barium–phosphate glasses. Canadian Journal of Physics, 90, 235–239. https://doi.org/10.1139/p2012-011

Li, Y., Chen, L., Chen, X., Hill, R., Zou, S., Wang, M., Liu, Y., Wang, J., & Chen, X. (2021). High phosphate content in bioactive glasses promotes osteogenesis in vitro and in vivo. Dental materials, 37(2), 272–283. https://doi.org/10.1016/j.dental.2020.11.017

Lilja, T. (2022). Luuta korvaavat komposiittimateriaalit kudosteknologian skaffoldeissa.

Lima, D. B., de Souza, M. A. A., de Lima, G. G., Ferreira Souto, E. P., Oliveira, H. M. L., Fook, M. V. L., & de Sá, M. J. C. (2020). Injectable bone substitute based on chitosan with polyethylene glycol polymeric solution and biphasic calcium phosphate microspheres. Carbohydrate polymers, 245, 116575–116575. https://doi.org/10.1016/j.carbpol.2020.116575

Marchi, Juliana. (2016). Biocompatible Glasses From Bone Regeneration to Cancer Treatment (1st ed. 2016.). Springer International Publishing. https://doi.org/10.1007/978-3-319-44249-5

Marie, P. J., Ammann, P., Boivin, G., & Rey, C. (2001). Mechanisms of action and therapeutic potential of strontium in bone. Calcified Tissue International, 69(3), 121–129. https://doi.org/10.1007/s002230010055

Massera, J., Petit, L., Cardinal, T., Videau, J. J., Hupa, M., & Hupa, L. (2013). Thermal properties and surface reactivity in simulated body fluid of new strontium ion-containing phosphate glasses. Journal of materials science. Materials in medicine, 24(6), 1407–1416. https://doi.org/10.1007/s10856-013-4910-9

Nandi, S. K. (2011). Development and Applications of Varieties of Bioactive Glass Compositions in Dental Surgery, Third Generation Tissue Engineering, Orthopaedic Surgery and as Drug Delivery System. IntechOpen. https://doi.org/10.5772/24942

National Center for Biotechnology Information (2024). PubChem Compound Summary for CID 6326975, Phosphorus pentoxide. Retrieved March 21, 2024 from https://pubchem.ncbi.nlm.nih.gov/compound/Phosphorus-pentoxide.

Ralston, S. H. (2021). Bone structure and metabolism. Medicine (Abingdon. 1995, UK ed.), 49(9), 567–571. https://doi.org/10.1016/j.mpmed.2021.06.009

Reznikov, N., Shahar, R., & Weiner, S. (2014). Bone hierarchical structure in three dimensions. Acta biomaterialia, 10(9), 3815–3826. https://doi.org/10.1016/j.actbio.2014.05.024

Robinson, T. E., Hughes, E. A. B., Eisenstein, N. M., Grover, L. M., & Cox, S. C. (2020). The Quantification of Injectability by Mechanical Testing. Journal of Visualized Experiments, 2020(159). https://doi.org/10.3791/61417

Romanò, C. L., Logoluso, N., Meani, E., Romanò, D., De Vecchi, E., Vassena, C., & Drago, L. (2014). A comparative study of the use of bioactive glass S53P4 and antibiotic-loaded calcium-based bone substitutes in the treatment of chronic osteomyelitis: A retrospective comparative study. The bone & joint journal, 96(6), 845–850. https://doi.org/10.1302/0301-620X.96B6.33014

Sadiasa, A., Sarkar, S. K., Franco, R. A., Min, Y. K., & Lee, B. T. (2014). Bioactive glass incorporation in calcium phosphate cement-based injectable bone substitute for improved in vitro biocompatibility and in vivo bone regeneration. Journal of biomaterials applications, 28(5), 739–756. https://doi.org/10.1177/0885328213478256

Schmidt-Bleek, K., Schell, H., Lienau, J., Schulz, N., Hoff, P., Pfaff, M., Schmidt, G., Martin, C., Perka, C., Buttgereit, F., Volk, H.-D., & Duda, G. (2014). Initial immune reaction and angiogenesis in bone healing. Journal of tissue engineering and regenerative medicine, 8(2), 120–130. https://doi.org/10.1002/term.1505

Sergi, R., Bellucci, D., & Cannillo, V. (2020). A review of bioactive glass/natural polymer composites: State of the art. Materials, 13(23), 1–38. https://doi.org/10.3390/ma13235560

Song, H.-Y., Esfakur Rahman, A. H. M., & Lee, B.-T. (2009). Fabrication of calcium phosphate-calcium sulfate injectable bone substitute using chitosan and citric acid. Journal of materials science. Materials in medicine, 20(4), 935–941. https://doi.org/10.1007/s10856-008-3642-8

Winkler, T., Sass, F. A., Duda, G. N., & Schmidt-Bleek, K. (2018). A review of biomaterials in bone defect healing, remaining shortcomings and future opportunities for bone tissue engineering: The unsolved challenge. Bone & joint research, 7(3), 232–243. https://doi.org/10.1302/2046-3758.73.BJR-2017-0270.R1

Ying, X., Cheng, S., Wang, W., Lin, Z., Chen, Q., Zhang, W., Kou, D., Shen, Y., Cheng, X., Rompis, F. A., Peng, L., & zhu Lu, C. (2011). Effect of Boron on Osteogenic Differentiation of Human Bone Marrow Stromal Cells. Biological trace element research, 144(1–3), 306–315. https://doi.org/10.1007/s12011-011-9094-x

Zreiqat, Hala., Dunstan, C. R., & Rosen, Vicki. (2015). A Tissue Regeneration Approach to Bone and Cartilage Repair (1st ed. 2015.). Springer International Publishing. https://doi.org/10.1007/978-3-319-13266-2